5-2021

Bioretention Cell Performance Under Shifting Precipitation Patterns Across the Contiguous United States

Matthew Weathers
mweath11@vols.utk.edu

To the Graduate Council:

I am submitting herewith a thesis written by Matthew Weathers entitled "Bioretention Cell Performance Under Shifting Precipitation Patterns Across the Contiguous United States." I have examined the final electronic copy of this thesis for form and content and recommend that it be accepted in partial fulfillment of the requirements for the degree of Master of Science, with a major in Environmental Engineering.

Jon M. Hathaway, Major Professor

We have read this thesis and recommend its acceptance:

Anahita Khojandi, John S. Schwartz

Accepted for the Council:
Dixie L. Thompson

Vice Provost and Dean of the Graduate School

(Original signatures are on file with official student records.)

Bioretention Cell Performance Under Shifting Precipitation Patterns Across the Contiguous United States

A Thesis Presented for the
Master of Science
Degree
The University of Tennessee, Knoxville

Matthew R. Weathers
May 2021

ABSTRACT

As climate change produces shifts in precipitation patterns, communities will need to understand how the performance of green stormwater infrastructure (GSI) may be impacted. Bioretention cells are one of the most commonly implemented forms of GSI for their ability to reduce peak discharge and filter pollutants and are a vulnerable component of stormwater infrastructure. Projections in future climate indicate that bioretention cells may be at risk of losing their existing function due to deviations in precipitation frequency and intensity. General circulation models (GCMs) downscaled to regional climate models (RCMs) can provide climate change projections at a high spatial resolution but often have a degree of bias introduced during the downscaling process. As such, an ensemble of 10 regional climate models and 17 locations across the contiguous United States were evaluated to provide the widest range of potential future outcomes. Bioretention cells were modeled using USEPA's Storm Water Management Model (SWMM) to compare observed and future performances. Observed climate data from 1999 to 2013 were gathered from NOAA's National Centers for Environmental Information data archive, and simulated future climate data from 2035 to 2049 were gathered from the North American Coordinated Regional Downscaling Experiment data archive. To reduce model bias, simulated future climate data was bias-corrected using the kernel density distribution mapping (KDDM) technique. Median annual rainfall and 99^{th} percentile rainfall event depths were projected to increase across all 17 locations while median drying period was projected to decrease for 11 locations, indicating fewer events with higher magnitudes of rainfall for a majority of locations. Correspondingly, bioretention cell performance decreased across all 17 locations. Relative percent changes in infiltration loss decreased between 4.0-24.0% across all 17 locations while overflow increased between 0.4-19.6% for 15 locations. Results suggest that bioretention cells in the

southern United States are at significant risk of losing their existing function while those in the Midwest and Northeast are at moderate risk. Bioretention cells in the western and northwestern United States performed the best under future climate scenarios but could still lose their existing function if unchanged. Most, if not all, bioretention cells across the contiguous United States will, therefore, require some degree of modification to maintain their existing function in the future. This study provides insight on future regional bioretention cell performance trends that can be used to add resiliency to stormwater infrastructure.

TABLE OF CONTENTS

LIST OF TABLES

LIST OF FIGURES

CHAPTER ONE
INTRODUCTION AND GENERAL INFORMATION

Introduction

The effects of anthropogenic activities on the Earth's climate are difficult to fully quantify, but the affiliated increased likelihood of extreme weather events (e.g., frequent floods, drought conditions, record-breaking temperatures) has been firmly documented (Masson-Delmotte et al. 2018; Kaufmann et al. 2011; Rosenzweig et al. 2008). According to the National Oceanic and Atmospheric Administration Global Surface Temperature Dataset (Zhang et al. 2018a), the last 5 years (2015-2019) and 8 of the last 10 years (2010-2019) have been the warmest years on record since global temperature records began in 1880. Additionally, using the NOAAGlobalTemp Dataset, Arguez et al. (2020) predicts there is a greater than 99% probability that this next decade (referring to 2019-2028) will be among the 10 warmest years on record; since publication of the article, 2019 has been ranked as the 2nd hottest year on record (Zhang et al. 2018a). Despite this understanding, identifying specific impacts of climate change can be challenging due to constantly varying regional weather patterns. Defined by temperature fluctuations and precipitation frequency, intensity, and duration, regional weather patterns vary significantly by location and season. To understand climate change impacts at the national scale, differences in regional climate perturbations must be explored and understood.

Increasingly frequent extreme precipitation events illustrate the need for demonstrable efforts to mitigate the worsening effects of climate change. Bishop et al. (2019) found a 40% increase in fall precipitation for the period 1895-2018 in the southeastern United States north of the Gulf of Mexico, with nearly all of the added precipitation occurring with an increased intensity. Additionally, the rapid acceleration of urban growth across the planet has led to a greater

percentage of urban areas becoming covered by impervious surfaces that disallow soil infiltration. Zhang et al. (2018b) showed that the extreme flooding caused by Hurricane Harvey in August 2017 was exacerbated due to both anthropogenic-induced climate change and the effects of increased urbanization in Houston, TX, USA.

One critical infrastructure directly affected by climate change is the stormwater management system. Mitigating the effects of climate change requires additional investment in stormwater infrastructure capable of handling future precipitation events. Stormwater infrastructure is typically broken into two categories, gray and green. Gray stormwater infrastructure is historically designed to move stormwater away from impervious urban areas as quickly as possible using curbs, gutters, drains, and piping. Green stormwater infrastructure (GSI), which relies on stormwater control measures (SCMs), is designed to imitate nature by allowing runoff to be slowed, infiltrated, and evapotranspired. While the majority of cities in the United States have historically relied more heavily on gray stormwater infrastructure, a significant push in the past 10 years has been made to incorporate more green stormwater infrastructure, which can provide some of the same benefits as gray stormwater infrastructure while promoting a more natural hydrologic cycle in urban areas and a slew of additional ecosystem and social services. Such SCMs are promoted as adding buffering capacity to urban watersheds, and thus resilience to climate change, reducing the need for increasing the capacity of grey infrastructure in response to more intense weather.

Bioretention cells, or rain gardens, are one of the most common types of GSI and provide a cost-effective way of reducing peak discharge, allowing natural infiltration, improving water quality, and improving the visual attractiveness of heavily urbanized areas. Bioretention cells built in the present day are designed using Intensity-Duration-Frequency (IDF) curves and design

storms of a targeted percentile based on historical rainfall data. These approaches are predicated on climate stationarity. However, the increased occurrences of extreme storm events indicate the Earth is currently experiencing a period of climate non-stationarity. Given that gray and green stormwater infrastructure work together as part of a larger network of stormwater infrastructure, determining if bioretention cells built in the present day are capable of handling future precipitation events is critical for the efficacy of stormwater infrastructure as a whole. Equally important, the hydrologic impacts of regional precipitation variability in the future need to be determined. If extreme precipitation events become more frequent in some areas but not others, then resources can be better allocated to locations that will experience the most significant effects of climate change.

This thesis assesses the ability of bioretention cells built in the present day to handle future precipitation events, and explores design modifications that may result in better system resilience to a changing climate. To conduct this study, 17 locations across the United States were selected based off their unique hydrologic region. Each location is representative of one region, with the 17 regions accounting for the vast majority of the United States. To model future precipitation, 10 Regional Climate Models (RCMs) have been selected from the North American Coordinated Regional Downscaling Experiment (NA-CORDEX) to provide the widest range of potential future precipitation outcomes (Mearns et al. 2017). While some research has been performed assessing a single bioretention cell's ability to handle future precipitation events (in a single location), almost no research has been performed comparing multiple locations across the United States. As such, this research seeks to address this knowledge gap. By maintaining the same bioretention cell design specification across all 17 locations with 10 RCMs per location (170 total model runs) the results may be compared directly to one another. Using this information, guidance will be provided on

which locations will have bioretention designs most adversely affected by climate change, and thus may require modifications to ensure the desired performance persists in the future.

Chapter two provides a literature review of climate change, climate data, urbanization, and hydrologic and hydraulic modeling software. Chapter three documents the locations selected for this study, data collection of observed and simulated climate data, bias-correction procedure selected, methodology used for modeling the bioretention cells, and bioretention cell performance indices. Chapter four displays the results from the analysis of the data, provides a discussion of the main findings, and provides recommendations for management strategies. Chapter five summarizes the entirety of the research and provides suggestions for future research.

CHAPTER TWO
LITERATURE REVIEW

Climate Change

The past two decades have provided a significant amount of research related to climate change impacts on the environment and, more specifically, the hydrologic cycle. The hydrologic cycle is responsible for the continuous circulation of water in the earth and atmosphere and consists of five primary components: precipitation, evapotranspiration, condensation, infiltration, and surface runoff. One of the most critical hydrologic design inputs generated from precipitation data is the intensity-duration-frequency (IDF) curve, which graphically represents the probability of a specific rainfall depth or intensity within a period of time (Dupont and Allen 2000), and are indicative of trends observed in rainfall time series. Historically, hydrologic engineering designs have relied on the stationarity of rainfall patterns, and thus IDF curves, but recent research has shown that this can no longer be assumed with a shift towards increasingly frequent intense storm events (Horton et al. 2010; Meehl et al. 2000; Milly et al. 2008; Pryor et al. 2009).

Shifting Precipitation Patterns

Using datasets from 182 stations across the contiguous United States, Karl and Knight (1998) noted a 10% increase in precipitation primarily due to heavy daily precipitation events with 53% of the added precipitation being attributable to the upper 10% of the precipitation distribution. Examining the period from 1948 to 2006, Madsen and Figdor (2007) reported a 24% increase in extreme precipitation events across the contiguous United States, ranging from a 14% decrease in Oregon to a more than 50% increase in Rhode Island, New Hampshire, Massachusetts, Vermont, New York, and Louisiana; Oregon was one of only three states (Oregon, Florida, and Arkansas) that showed a decrease in the frequency of extreme precipitation events, and the only state of the

three to reach statistical significance. Olsson et al. (2009) performed a case study in Kalmar City, Sweden, and found that while total rainfall might decrease peak intensity will increase overall with an estimated 20 to 30% increase in the summer and an estimated 50 to 60% increase in the autumn by the year 2100. Kuo et al. (2015) performed a case study in central Alberta, Canada, predicting an increase in both the intensity and frequency of short duration storm events with an 84.9% increase in the projected intensity of sub-hourly storm events by the 2080s. Mailhot et al. (2007) performed a similar case study in southern Quebec, Canada, predicting the return periods of 2- and 6-hr events to halve by 2070. Similarly, Kirtman et al. (2013) notes that the global frequency and intensity of heavy precipitation will likely increase on average, and Prein et al. (2017) projects up to a 400% increase in the frequency of extreme precipitation events across almost the entirety of North America by 2100.

Clausius-Clapeyron Relationship

One of the potential causes of shifting rainfall trends is the Clausius-Clapeyron (C-C) relationship, which relates the increased moisture-holding capacity in the atmosphere to the temperature and may be approximated as 7%/°C (Trenberth et al. 2003). As of 2017, the Intergovernmental Panel on Climate Change (IPCC) reported that anthropogenic activities have led to an approximate increase of 1°C of global warming since pre-industrial levels, likely reaching 1.5°C between 2030 and 2052 if greenhouse gas emissions continue to increase at the current rate (Masson-Delmotte et al. 2018). This indicates that the moisture-holding capacity in the atmosphere has increased by approximately 7% since pre-industrial levels and could increase to 10.5% by 2052. It must be noted that the Clausius Clapeyron relationship varies by temperature (e.g., ~7.3%/°C at 0°C, 6.2%/°C at 20°C) and, therefore, also varies by latitude (Utsumi et al. 2011). A number of studies have explored the validity of the C-C relationship in a range of locations using

observed data. Schroeer and Kirchengast (2018) investigated temperature sensitivities of precipitation events at sub-hourly (10-min), hourly, and daily temporal resolutions in south-eastern Austria using data gathered from 189 stations covering April to October, 2014, and found that 10-min peak intensities increased with temperature greater than the C-C rate (>7%/°C); hourly peak intensities increased with temperature less than the C-C rate (<7%/°C); and daily peak intensities decreased with temperature. Similarly, using observed climate data in western Europe ranging from 1950 to 2009, Lenderink and Meijgaard (2010) investigated the relationship between hourly precipitation extremes (99^{th} and 99.9^{th} percentiles of events) and daily mean temperatures and found that four independent data sources confirmed a scaling relationship double the C-C rate (14%/°C) above 10°C. However, the C-C equation was not as explanatory in some other locations. Investigations by Ivancic and Shaw (2016) and Westra et al. (2014) indicated that the C-C rate underpredicts the increase in hourly and sub-hourly extreme precipitation in the mid-latitudes. Likewise, Donat et al. (2016) reported that the Clausius-Clapeyron relationship is only accurate in dry regions (e.g., central and northeast Asia, central Australia, northwestern North America, north and southwestern Africa) with no statistically significant relationship present in wet regions (e.g., Southeast Asia, India, eastern South America, southeastern United States, Europe). While there is debate regarding C-C scaling rate, the general consensus among climate researchers is that extreme precipitation events are becoming more frequent in most parts of the globe and are in part due to the Clausius-Clapeyron relationship (Berg et al. 2013; Fischer and Knutti 2016; Kendon et al. 2014; Wang et al. 2017a).

Climate Data

Climate change uncertainty has led to a range of representative concentration pathway (RCP) scenarios being produced by the IPCC (Pachauri et al. 2014) to indicate the range of

potential greenhouse gas concentration trajectories, and subsequent climate change impacts, which include a best-case scenario (RCP2.6), two intermediate scenarios (RCP4.5 and RCP6.0), and a worst-case scenario (RCP8.5). RCP2.6 and RCP4.5 scenarios indicate that global warming will not increase above 2℃ since pre-industrial levels by 2100 with medium confidence, while RCP6.0 and RCP8.5 scenarios indicate that global warming will increase above 2℃ since pre-industrial levels by 2100 with high confidence (Pachauri et al. 2014). Using the RCP scenarios produced by the IPCC (Pachauri et al. 2014), general circulation models (GCMs) and regional climate models (RCMs) are used to produce a range of simulated climate data to approximate future changes in global- and local-scale climate. GCMs are mathematical models used to simulate global climate by representing the physical processes in the atmosphere and ocean (IPCC 2013). GCMs provide a coarse view of climate, typically ranging from 250 to 600km grids, and, as such, are not ideal for modeling local climate. RCMs provide much finer resolution than GCMs, as fine as 12km grids, allowing for more accurate representation of local climate. However, production of RCMs requires downscaling of GCMs, often introducing a degree of bias during the downscaling process.

Bias-Correction

Due to bias introduced during the downscaling process and inherent model bias, bias-correction procedures must be applied to more accurately align modeled climate data with observed climate data. Stephens et al. (2010) compared five different weather prediction, climate, and global cloud "resolving" models and found that all models overproduced precipitation frequency by a factor of two while underproducing precipitation intensity compared to observed precipitation data. Comparing projected climate data (2021-2050) from 11 RCMs to observed climate data (1961-1990) for five catchments in Sweden, Teutschbein and Seibert (2012) evaluated six bias-correction methods, linear scaling, local intensity scaling, power transformation, variance

scaling, distribution mapping, and the delta-change approach. Results showed that all bias-corrected data more accurately reflected observed data than non-bias-corrected data with distribution mapping performing the best overall. Distribution mapping corrects RCM-simulated data by fitting a transfer function to the simulated data to more accurately reflect the patterns of the observed data while preserving short temporal variability (Sennikovs and Bethers 2009).

Kernel Density Distribution Mapping

A novel non-parametric technique known as kernel density distribution mapping has become increasingly popular in the past five years (Biglarbeigi et al. 2020; Lazante et al. 2019; McGinnis and Mearns 2016; Oleson et al. 2018; Tirpak et al. 2021) due to its ease of implementation, accurate bias-correction, and existing knowledge base from kernel density estimation methods (Sheather 2004; Solaiman and Simonovic 2011). McGinnis et al. (2015) evaluated six distribution mapping techniques, probability mapping (PMAP), order statistic difference correction (OSDC), empirical CDF mapping (ECDF), quantile mapping (QMAP), asynchronous regional regression modeling (ARRM), and kernel density distribution mapping (KDDM), and found that the KDDM technique performed best overall. Using KDDM to bias-correct simulated historic (1983-2014) and future (2020-2059) hourly precipitation and daily temperature data for 17 locations across the United States, Cook et al. (2019) reported a major benefit of the KDDM method being its ability to correct the statistical distribution of the simulated data while maintaining the temporal distribution of rainfall intensity in bias-corrected data.

Climate Data Studies

RCMs and GCMs have been used extensively to assess future hydrologic issues. For example, Ault et al. (2014) analyzed the output from 27 GCMs and 3 representative concentration pathway (RCP) scenarios (RCP2.6, RCP4.5, and RCP8.5) and found a 70 to 90% likelihood of a

decade-scale megadrought in the US Southwest between 2050 and 2100. Using 26 GCMs and 2 RCP scenarios (RCP2.6 and RCP8.5), Jhong and Tung (2018) investigated changes in precipitation extremes from 2020 to 2100 in the Shih-Men reservoir watershed of Taiwan and found an increased likelihood of heavy precipitation events and an increased number of consecutive wet days and dry days, leading a greater likelihood of both flood and drought conditions. Lastly, using 7 global impact models (GIMs) driven by 5 GCMs with 4 RCP scenarios (RCP2.6, RCP4.5, RCP6.0, and RCP8.5), Prudhomme et al. (2014) reported that under RCP8.5 Southern Europe, the Middle East, the Southeast United States, Chile, and South West Australia are particularly likely to experience droughts and water security issues by the year 2100. Comparing observed total daily precipitation data from the past 50- to 100-years with three general circulation model (GCM) projections, Groisman et al. (2005) analyzed changes in intense precipitation events (top 0.3% for daily precipitation events) for over half of the Earth's land area – focusing on the contiguous United States, Mexico, Brazil, Russia, Eastern Europe, South Africa, and Australia – and found an increased probability of intense precipitation events in extratropical regions. Examining 34 US cities and an ensemble of RCMs, Cook et al. (2020) showed that shorter, hourly storms will become both more variable and frequent than longer, daily storms between 2020 and 2099.

Urbanization

The detrimental effects of human-induced climate change are compounded due to increased urbanization worldwide (Bounoua et al. 2015; Ezber et al. 2007; Garschagen and Romero-Lankao 2015; Huong and Pathirana 2013; Kalnay and Cai 2003; Leopold 1968; Mahmoud and Gan 2018; Nelson and Palmer 2007; Nelson et al. 2009; Pielke et al. 2002). According to the United Nations (2018), from the year 1900 to the year 2016 the percentage of humans living in urban areas increased from 16.4 to 54.4%, more than tripling the number of

people in urban areas. In that same time period, urban growth in the United States increased from 40.0 to 81.9%, more than doubling. Urbanization is accompanied by a reduction in pervious surfaces (Schueler et al. 2009; Shuster et al. 2005) resulting in increased runoff and flooding (Chen et al. 2017; Du et al. 2012; Perry and Nawaz 2008; Suriya and Mudgal 2012), increased nonpoint source pollution (Bhaduri et al. 2000; O'Driscoll et al. 2010; Tang et al. 2005; Tong and Chen 2002), and urban stream syndrome (Walsh et al. 2005, 2012), in which urban runoff delivered to streams causes the degradation of waterways and biodiversity.

Urbanization Studies

The tangible impacts of urbanization have been shown in multiple studies, including Roy et al. (2005), where a positive correlation was reported between increased impervious areas and altered storm flows in summer months, leading to a decrease in the diversity of endemic fish species. Similarly, due to a projected increase in urban land use from 50 to 94% between 1992 and 2030 in the City of Normal-Sugar Creek Watershed in Central Illinois, USA, Ahiablame and Shakya (2016) found a greater than 30% increase in average annual runoff and flood events. Modelling a watershed near the O'Hare International Airport, Chicago, USA, Bhaduri et al. (2001) predicted a linear relationship between average annual runoff and increasing imperviousness – assuming a 10% increase in imperviousness resulted in an increase between 6.1 to 10.2% in annual average runoff. To remediate these impacts, researchers such as Gunn et al. (2012) have begun to look at design solutions, comparing pre-development and post-development hydrologic indices for three subdivisions – one designed with extensive conservation principles (e.g., little disruption of natural soils and forests, minimal increase in impervious cover, stormwater control ponds, additional trees), one designed with typical development principles (e.g., increased impervious cover, soil compaction due to construction), and one designed with a mix of conservation and

typical development principles (e.g., increased impervious cover, swales, additional trees) – in Lafayette, Indiana, USA. The subdivision designed with conservation principles performed better post-development (32% reduction in annual runoff, 237% increase in time of concentration) while both the typical and mixed subdivisions performed worse post-development resulting in increased average annual runoff (60% and 52%, respectively) and reduced time of concentration (20% and 17%, respectively).

Green Stormwater Infrastructure

Green stormwater infrastructure, or low impact development (LID) as explored by Gunn et al. (2012), is becoming more frequently utilized in urban areas to assist and supplant existing gray stormwater infrastructure to bring resilience to anthropogenic-induced climate change (Chan et al. 2018; Eckart et al. 2017; Mei et al. 2018). As an example, using 1961-1990 as a baseline, Gill et al. (2007) found that an additional 10% GSI in Greater Manchester, England, UK, could keep max surface temperatures at or below baseline temperatures up to, but excluding, the modeled 2080s high. Exploring the hydrologic benefits of LID, Dietz and Clausen (2008) compared pre-development and post-development annual runoff and pollutant export (total phosphorus (TP) and total nitrogen (TN)) for two subdivisions – one 2.0ha traditional subdivision with 17 lots designed using typical development principles and one 1.7ha LID subdivision with 12 lots designed with bioretention cells, grassed swales, an Ecostone® paver road, and a collection of BMPs (e.g., locating and seeding stockpiles to prevent sediment loss, hay bales, silt fences, earthen berms, post-storm maintenance) – in Waterford, Connecticut, USA. Post-development annual runoff and pollutant export increased logarithmically with increase in impervious coverage (e.g., runoff increased from 0.1cm to over 50cm) for the traditional subdivision while post-development annual runoff and pollutant export remained unchanged for the LID subdivision.

Bioretention Cell

One of the most commonly implemented and studied types of GSI has become the bioretention cell, which consists of layers of gravel, soil, sand, organic matter, plants, and filter strips (TDEC 2014). Bioretention cells provide removal of total suspended solids (TSS) and pollutants (TN, TP) (Davis et al. 2001, 2003, 2006; Line and Hunt 2009; Luell et al. 2011) while reducing runoff volume and peak discharge (Ahiablame et al. 2012; Bonneau et al. 2020; Chapman and Horner 2010; Dietz 2007; Dietz and Clausen 2005; Moore et al. 2016; Schlea et al. 2014). Monitoring three bioretention cells built in northeast Ohio, USA, from May to November 2014, covering 28 precipitation events, Winston et al. (2016) reported runoff reductions ranging from 36 to 59% and peak flow reductions ranging from 24 to 96% for events exceeding 1-year, 5-minute rainfall intensity. Monitoring two bioretention cells constructed on the University of Maryland campus in College Park, Maryland, USA for nearly two years, covering 49 runoff events, Davis (2008) found that 18% of events were small enough to be fully captured by the bioretention cell without outflow with mean peak flow reductions of 49% and 58% for all other events.

Hydrologic and Hydraulic Modeling Software

Prior to design completion and subsequent construction, hydrologic and hydraulic (H&H) modeling software are commonly used to optimize the design and performance of stormwater infrastructure. Coupled H&H modeling software combine precipitation frequency, intensity, and duration from hydrologic models (e.g., US Army Corps of Engineers Hydrologic Engineering Center Hydrologic Modeling System) with the physical characteristics of open channel flow from hydraulic models (e.g., US Army Corps of Engineers Hydrologic Engineering Center River Analysis System). H&H modeling software provide an additional measure of certainty for engineers, architects, and urban planners for ensuring that an urban area is capable of safely

handling and passing present and future precipitation events. An array of H&H modeling software exists due to the individual requirements of stormwater infrastructure projects (e.g., some projects require simple, neighborhood-size models while other projects require robust, metro-size models).

Modeling GSI

Hathaway et al. (2014) used DRAINMOD to model four bioretention cells, with two in both Rocky Mountain and Nashville, North Carolina, USA, for two RCP scenarios (RCP4.5, RCP8.5). Comparing historic (2001-2004) performance with projected performance (2055-2058), results showed that the frequency and volume of overflow could increase significantly for projected scenarios, requiring an additional storage of between 9 and 31cm to restrict annual overflow. Using the MIKE URBAN model, Berggren et al. (2012) performed a case study in a small suburb in southeast Sweden to determine the hydraulic performance of the existing urban drainage system for the present and three future periods (2011-2040, 2041-2070, and 2071-2100). Results showed that the model underestimated peak flows by 13% on average but was accurate overall in its prediction of increased future flood frequency and duration. Semadeni-Davies et al. (2008) performed a similar study in Helsingborg, south Sweden, using a combination of two H&H models, MIKE SHE for permeable surfaces and MOUSE (MOdel of Urban SEwers) for impervious surfaces and channel flow, to assess the combined effects of climate change and urbanization on urban drainage. Alteration of input climate data and model parameters allowed the models to assess a range of future climate and urbanization scenarios. Results showed that under the future best-case scenario urban drainage could be exacerbated by increased precipitation leading to increased surface runoff while the worst-case scenario could lead to increased peak flow volumes and flood risk, both of which could be managed through the installation of sustainable urban drainage systems (SUDS).

Modeling GSI Using SWMM LID Controls

One of the most commonly used H&H modeling software is the USEPA's Storm Water Management Model (SWMM) which provides dynamic rainfall-runoff relationships for single-event and long-term simulations (Denault et al. 2006; Gironás et al. 2009). SWMM version 5.1 comes standard with LID controls, allowing for explicit modeling of rain gardens, bioretention cells, vegetative swales, infiltration trenches, green roofs, rooftop disconnection, rain barrels, and porous pavement (Rossman 2015). Using PCSWMM – SWMM incorporated within a graphical user interface – Lucas and Sample (2015) compared two conventional gray stormwater infrastructure scenarios with two GSI scenarios using multiple LID controls (e.g., green roofs, infiltration trenches, porous pavement, and bioretention cells) for two separate years (one year with average rainfall depth and intensity and one year with higher intensity due to climate change). Results showed that the two GSI scenarios performed better than the two gray stormwater infrastructure scenarios for both years with relative performance improvements during the climate change year. Similarly, using SWMM LID controls to model bioretention cells in two urban catchments in Singapore using 16 model ensembles and 4 RCP scenarios (RCP2.6, RCP4.5, RCP6.0, and RCP8.5) from 2040 to 2059, Wang et al. (2017b) reported that LID is effective at reducing peak runoff and can improve water quality. Using SWMM LID controls, Wang et al. (2019a) performed a case study in Guangzhou, China, to assess the effectiveness of bioretention cells for the future period 2040 to 2059. Results showed that the bioretention cells were effective in controlling peak runoff for small storms of short duration but were unable to replace conventional gray stormwater infrastructure for large storms of long duration.

Knowledge Gaps and Research Objectives

The majority of studies examining the performance of bioretention cells under future precipitation events have focused on a single bioretention cell in a single location and a narrow range of climate change scenarios. Additionally, future climate data used for bioretention cell modeling are typically either not bias-corrected or undergo a simplistic bias-correction procedure. As such, bioretention cell performance comparisons between different locations have required comparisons between different studies. Due to the potential use of different sources of climate data, bias-correction procedures, modeling methods, and bioretention cell design characteristics, a degree of inaccuracy may be introduced in any conclusions made from the comparisons. A knowledge gap, therefore, exists in comparing a single bioretention cell's ability to handle future precipitation events across multiple locations while using the same source of climate data, bias-correction procedure, modeling method, and bioretention cell design characteristics.

This study will address the knowledge gap by maintaining the same bioretention cell design characteristics in SWMM across an ensemble of US locations and model scenarios using the same sources of climate data and bias-correction procedure. The methodology used in this study will allow for direct comparison of bioretention cell performance across all US locations and model scenarios selected, which has yet to be done in a previous study at this scale.

CHAPTER THREE
DATA COLLECTION AND METHODOLOGY

Data Collection

To provide the widest range of potential future outcomes, an ensemble of 17 US locations and 10 model scenarios were used in this study. Observed climate data were acquired from NOAA's National Centers for Environmental Information (NCEI) data archive to allow for bias-correction of future simulated climate data and characterization of historical bioretention function. Simulated historic and future climate data were acquired from the North American Coordinated Regional Downscaling Experiment (NA-CORDEX) data archive.

Bukovsky Climate Regions

Since the primary purpose of this study was to investigate changing hydrologic patterns nationally and their impact on stormwater management controls, the 17 US locations were selected based on their unique hydrologic region. As such, the Bukovsky climate map was used due to the hydrologic classification of climate regions (Bukovsky et al. 2019). The most frequently used climate classification systems, Köppen (1900) and Thornthwaite (1984), are highly vegetation-based and hydrologically oversimplify the eastern United States while overcomplicating the western United States. The Bukovsky climate map, however, groups regions by hydrologic similarity, accounting for average temperature and rainfall as well as seasonal occurrences, such as the North American monsoon (Bukovsky 2011). Using the same cities as Cook et al. (2019), one representative city was present in the analysis from each climate region in the contiguous United States. Table 1 provides the characteristics of all 17 locations used in this study along with their accompanying NOAA NCEI station name used for observed climate data collection. Fig. 1 displays the 17 representative locations and hydrologic regions of the contiguous United States.

Table 1. Characteristics of US cities used in this study

City	State	Bukovsky Region	Latitude[a]	Longitude[a]	NOAA NCEI Station Name
Amarillo	TX	C. Plains (11)	35.2220°	-101.8313°	AMARILLO AIRPORT TX US
Boise	ID	Great Basin (9)	43.6150°	-116.2023°	BOISE AIR TERMINAL ID US
Boston	MA	North Atlantic (20)	42.3601°	-71.0589°	BOSTON MA US
Boulder	CO	S. Rockies (8)	40.0169°	-105.2796°	BOULDER 2 CO US
Charlotte	NC	Mid Atlantic (19)	35.2271°	-80.8431°	CHARLOTTE DOUGLAS AIRPORT NC US
Chicago	IL	Great Lakes (14)	41.8832°	-87.6324°	CHICAGO OHARE INTERNATIONAL AIRPORT IL US
El Paso	TX	Mezquital (6)	31.7619°	-106.4850°	EL PASO INTERNATIONAL AIRPORT TX US
Fargo	ND	N. Plains (10)	46.8772°	-96.7898°	FARGO HECTOR INTERNATIONAL AIRPORT ND US
Memphis	TN	Deep South (16)	35.1495°	-90.0490°	MEMPHIS INTERNATIONAL AIRPORT TN US
Missoula	MT	N. Rockies (7)	46.8721°	-113.9940°	MISSOULA INTERNATIONAL AIRPORT MT US
New Orleans	LA	Southeast (17)	29.9511°	-90.0715°	NEW ORLEANS AIRPORT LA US
Phoenix	AZ	Southwest (5)	33.4484°	-112.0740°	PHOENIX AIRPORT AZ US
Pittsburgh	PA	Appalachia (15)	40.4406°	-79.9959°	PITTSBURGH ASOS PA US
Portland	OR	Pacific NW (3)	45.5122°	-122.6587°	PORTLAND INTERNATIONAL AIRPORT OR US
San Antonio	TX	S. Plains (12)	29.4241°	-98.4936°	SAN ANTONIO INTERNATIONAL AIRPORT TX US
San Jose	CA	Pacific SW (4)	37.3348°	-121.8881°	SAN JOSE CA US
St. Louis	MO	Prairie (13)	38.6270°	-90.1994°	ST LOUIS LAMBERT INTERNATIONAL AIRPORT MO US

[a]Values provided by latlong.net

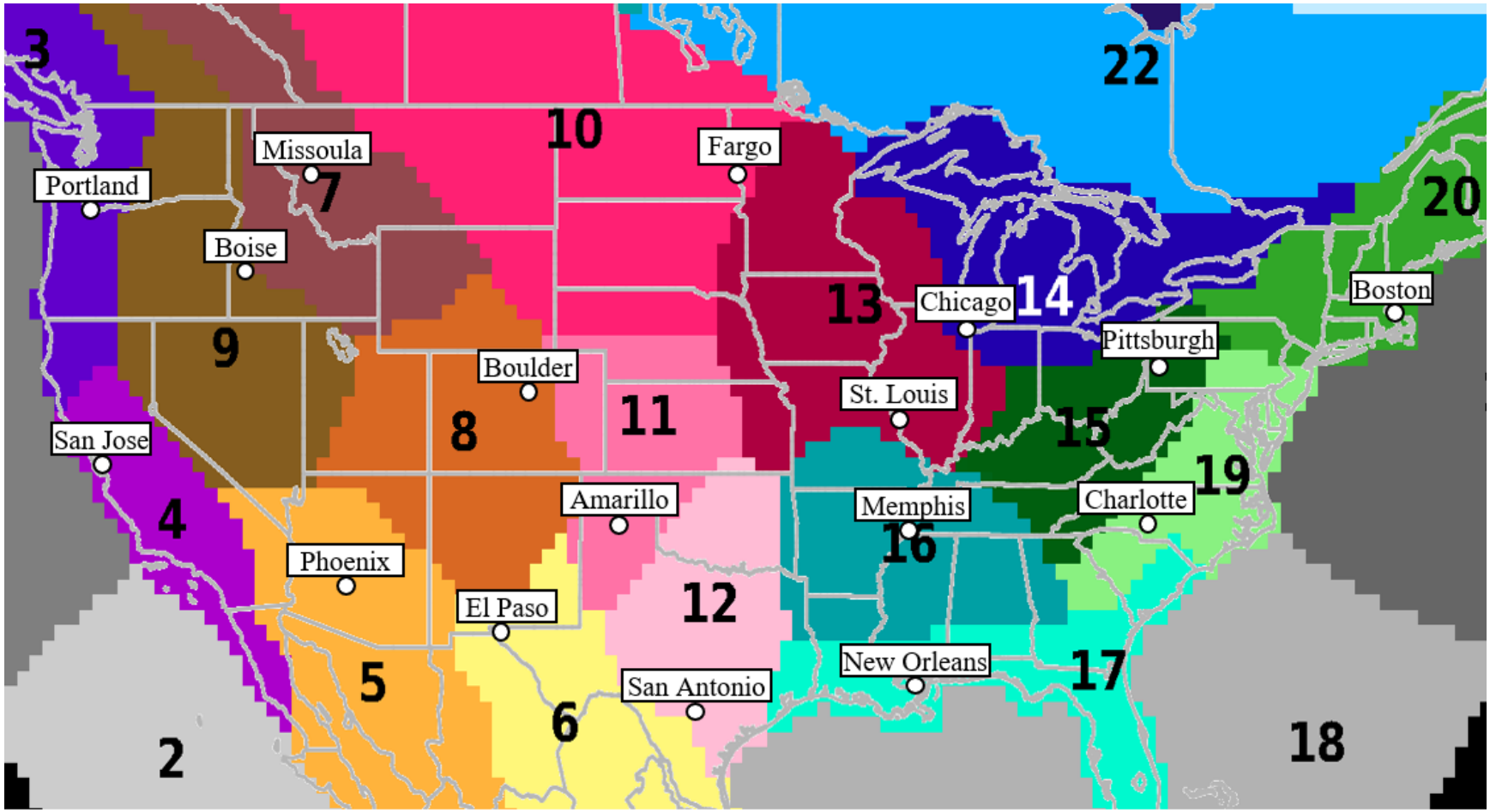

Fig. 1. Bukovsky climate map showing the 17 representative locations and hydrologic regions of the contiguous United States (Bukovsky 2011)

NOAA NCEI Observed Climate Data

Observed daily temperature (maximum and minimum) and hourly precipitation data from January 1, 1999, to December 31, 2013, were gathered from NOAA's NCEI for all 17 locations (NOAA 2016). The 15-year period was selected to fully capture the year-to-year variability of precipitation and temperature data. This time frame was chosen due to 2013 being the most recent year on record for hourly precipitation in the database. Hourly precipitation data was used in this study due to it being the finest available temporal resolution. Due to the speed of the rainfall-runoff relationship in urban areas caused by impervious surfaces, the highest available temporal resolution for precipitation must be used to accurately model the relationship.

The 17 NOAA NCEI stations shown in Table 1 were selected based off the availability of continuous climate data for the time range specified and close proximity to the selected cities. Table 2 provides the parameters included for NOAA NCEI climate data queries. In rare cases of missing data, a value of "99999" was provided in place of the climate data by the NOAA NCEI data archive. The value of "99999" was subsequently replaced by averaging the three preceding and three following hours for precipitation (e.g., "99999" at 16:00 was corrected by averaging 13:00-15:00 with 17:00-19:00) or days for temperature (e.g., "99999" on March 4 was corrected by averaging March 1-3 with 5-7).

NA-CORDEX Simulated Climate Data

Covering the majority of North America, the NA-CORDEX data archive provides simulated climate data from a range of RCMs produced using boundary conditions from GCMs in the Coupled Model Intercomparison Project Phase 5 (CMIP5) (Mearns et al. 2017). As recommended by Bukovsky and Mearns (2020), all ten NA-CORDEX climate models with available simulated hourly precipitation data were used for this study to provide the most

Table 2. Characteristics of NOAA NCEI Climate Data (NOAA 2016)

Hourly Precipitation Parameter	Description
STATION	Station identification number
STATION_NAME	Station location name
ELEVATION	Elevation above mean sea level (ft)
LATITUDE	Northern hemisphere location value (°)
LONGITUDE	Western hemisphere location value (°)
DATE	Year, month, day, and hour
HPCP	Precipitation amount (in)
Daily Temperature Parameter	**Description**
STATION	Station identification number
STATION_NAME	Station location name
ELEVATION	Elevation above mean sea level (ft)
LATITUDE	Northern hemisphere location value (°)
LONGITUDE	Western hemisphere location value (°)
DATE	Year, month, day, and hour
TMAX	Daily maximum near-surface air temperature (°F)
TMIN	Daily minimum near-surface air temperature (°F)

comprehensive range of potential future outcomes. Due to the limited availability of simulated hourly precipitation data, only one RCP4.5 scenario was evaluated while nine RCP8.5 scenarios were evaluated. Table 3 provides the characteristics for each NA-CORDEX climate model used in this study resulting in an ensemble of two RCP scenarios, four GCMs, three RCMS, and two spatial resolutions. Both historic simulated climate data from January 1, 1999, to December 31, 2013, and future simulated climate data from January 1, 2035, to December 31, 2049, were acquired to allow for bias-correction and SWMM modeling.

Table 4 provides the parameters included for NA-CORDEX hourly precipitation and daily temperature data queries. Following the download of all NA-CORDEX simulated climate data, two data issues had to be corrected prior to bias-correction. The first data issue was the lack of leap year climate data for six models (Models 1-4 and 9-10 from Table 3), which occurred four times in both the historic (2000, 2004, 2008, and 2012) and future (2036, 2040, 2044, and 2048) climate data ranges. Hourly precipitation values for February 29 of those years were produced by averaging the values at the same hour on the preceding and following days (e.g., for February 29 at 13:00, averaging February 28 at 13:00 and March 1 at 13:00). Daily temperature values for February 29 of those years were produced by averaging the values on the three preceding and three following days (e.g., February 26-28 averaged with March 1-3). The second data issue affected the temperature values of three models (Models 3-5 from Table 3) during the December 2005 time period with erroneous temperature values being denoted by the value “10,000,000”. Temperature values were corrected by averaging the values on the same day for the two preceding and two following years (e.g., December 1, 2005, was corrected by averaging December 1 for 2003, 2004, 2006, and 2007). To enable bias correction, hourly precipitation values were converted from kg m^{-2} s^{-1} to inches, and daily temperature values were converted from Kelvin to degrees Fahrenheit.

Table 3. Characteristics of NA-CORDEX climate models used in this study[a]

Model	RCP	GCM	RCM	Spatial Resolution
1	4.5	CanESM2	CanRCM4	50km
2	8.5	CanESM2	CanRCM4	50km
3	8.5	GFDL-ESM2M	WRF	25km
4	8.5	GFDL-ESM2M	WRF	50km
5	8.5	HadGEM2-ES	WRF	25km
6	8.5	HadGEM2-ES	WRF	50km
7	8.5	MPI-ESM-LR	RegCM4	25km
8	8.5	MPI-ESM-LR	RegCM4	50km
9	8.5	MPI-ESM-LR	WRF	25km
10	8.5	MPI-ESM-LR	WRF	50km

[a]NA-CORDEX data provided by Mearns et al. (2017)

Table 4. Characteristics of NA-CORDEX climate data used in this study[a]

Hourly Precipitation Parameter	Description
time	Year, month, day, and hour
latitude[unit="degrees_north"]	Northern hemisphere location value (°)
longitude[unit="degrees_east"]	Western hemisphere location value (°)
pr[unit="kg m^{-2} s^{-1}"]	Hourly precipitation flux (IPCC units)
Daily Temperature Parameter	**Description**
time	Year, month, day, and hour
latitude[unit="degrees_north"]	Northern hemisphere location value (°)
longitude[unit="degrees_east"]	Western hemisphere location value (°)
tasmax/tasmin[unit="K"]	Daily maximum/minimum near-surface air temperature (K)

[a]NA-CORDEX data provided by Mearns et al. (2017)

Methodology

Following climate data compilation, bias-correction and SWMM modeling were performed. Bias-correction of the simulated climate data was performed using the kernel density distribution mapping (KDDM) procedure (McGinnis et al. 2015). Following bias-correction, the SWMM model was designed and run using the observed climate data and the bias-corrected future climate data. The performance indices of infiltration loss, underdrain pipe outflow, and overflow were compiled for each model run to allow for comparison in the results and recommendations chapter.

KDDM Bias-Correction

The KDDM bias-correction procedure was selected due its accuracy, ease of implementation, and overall performance compared to other bias-correction procedures (McGinnis et al. 2015). Kernel density distribution mapping applies a set of bias-correction steps to more accurately align the distribution of simulated climate data with the distribution of observed climate data. Due to climate models over predicting the frequency of precipitation (Stephens et al. 2010), the excess drizzle was first removed from simulated precipitation data by setting hourly precipitation volumes below a minimum threshold to zero in order to match the wet/dry ratio of observed precipitation data (McGinnis and Mearns 2016). Following dedrizzling, nonparametric estimates of the underlying probability density functions (PDFs), similar to smooth, non-discrete histograms, were produced for the observed and simulated precipitation datasets. Each value in the simulated precipitation datasets is individually adjusted using kernel density estimation (KDE) by summing copies of the Gaussian kernel function (McGinnis et al. 2015; Sheather 2004). The resulting PDFs were integrated using the trapezoidal rule to approximate cumulative distribution functions (CDFs). A transfer function was then created by fitting a spline between the

corresponding quantiles for the inverse CDF of the observed precipitation data and the forward CDF of the simulated precipitation data (McGinnis et al. 2015; Panofsky and Brier 1968). Lastly, the transfer function was applied to both the historic and future simulated precipitation data for bias-correction. KDDM bias-correction of the simulated temperature data followed the same steps as the precipitation bias-correction, with the exception of the dedrizzling step, and was performed on a monthly basis to account for seasonal variability (McGinnis et al. 2015).

Due to the September 2013 floods in Boulder, CO, which led to 9.08in of rainfall on September 12 (NOAA 2016) and nearly doubled the previous daily record of 4.8in (Hamill 2014), using the full observed hourly precipitation dataset led to extremely erroneous bias-corrected hourly precipitation data. According to NOAA's National Weather Service Precipitation Frequency Data Server (2017), the 24-hr, 1000-year precipitation depth for Boulder, CO, is 8.16in, 0.92in less than the rainfall on September 12, 2013, further illustrating the rarity of the precipitation event. Cook (2018) reported that extreme values in observed data used to bias-correct simulated data may lead to inaccurate annual maximum values if observed outliers are not removed prior to KDDM bias-correction. As such, observed hourly precipitation data from September 9, 2013, to December 31, 2013, were removed from the Boulder, CO, observed hourly precipitation data, which significantly improved the accuracy of the bias-corrected hourly precipitation data.

KDDM bias-correction of the simulated hourly precipitation and daily temperature data was performed using the R package "climod" (McGinnis 2018) with the steps outlined in Fig. 2. Performing the same statistical analysis as Tirpak et al. (2021), the Wilcoxan rank sum test confirmed the statistical similarities between the observed climate data distribution and the bias-corrected climate data distribution for all 10 models across all 17 locations (R Core Team 2020). The bias-corrected future climate data was, therefore, confirmed as a suitable for subsequent

SWMM modeling. Following bias-correction, an implausibly high precipitation amount was noted in the bias-corrected future dataset in El Paso using Model 6 (378.6in in 4 hours). The precipitation amount was subsequently removed and set to 0in for the 4-hour time period, subsequently producing future precipitation statistics more in line with the other nine models.

SWMM Modeling

USEPA's Storm Water Management Model (SWMM) Version 5.1 was used in this study for its ability to provide dynamic rainfall-runoff relationships for long-term simulations and directly model bioretention cells using the LID Control Editor (Rossman 2015). The SWMM model consisted of a 1-acre (43,560 ft^2) subcatchment, a bioretention cell, a rain gage, and an outlet. Detailed design characteristics for the subcatchment are shown in Table 5. The subcatchment was designed with 100% impervious cover to represent a common, yet hypothetical impervious surface in a city, such as a parking lot. As such, a Manning's n value of 0.01 was selected for the impervious surface to account for the hydraulic efficiency of the subcatchment (Arcement and Schneider 1989). All runoff from the subcatchment was routed directly to the bioretention cell. While bioretention cell design guidelines do vary slightly by state and, more significantly, by region, bioretention cell characteristics were kept constant for all locations and models to ensure the only independent variable was climate (observed and bias-corrected future) allowing for relative changes in bioretention cell performance to be assessed. Bioretention cell design characteristics were based off the Baseline bioretention design scenario used by Tirpak et al. (2021) and incorporated design recommendations from the Tennessee Department of Conservation (TDEC 2014), the Minnesota Stormwater Steering Committee (MSSC 2006), the Knox County, Tennessee Stormwater Management Manual (County 2008), and the Storm Water Management Model User's Manual Version 5.1 (Rossman 2015).

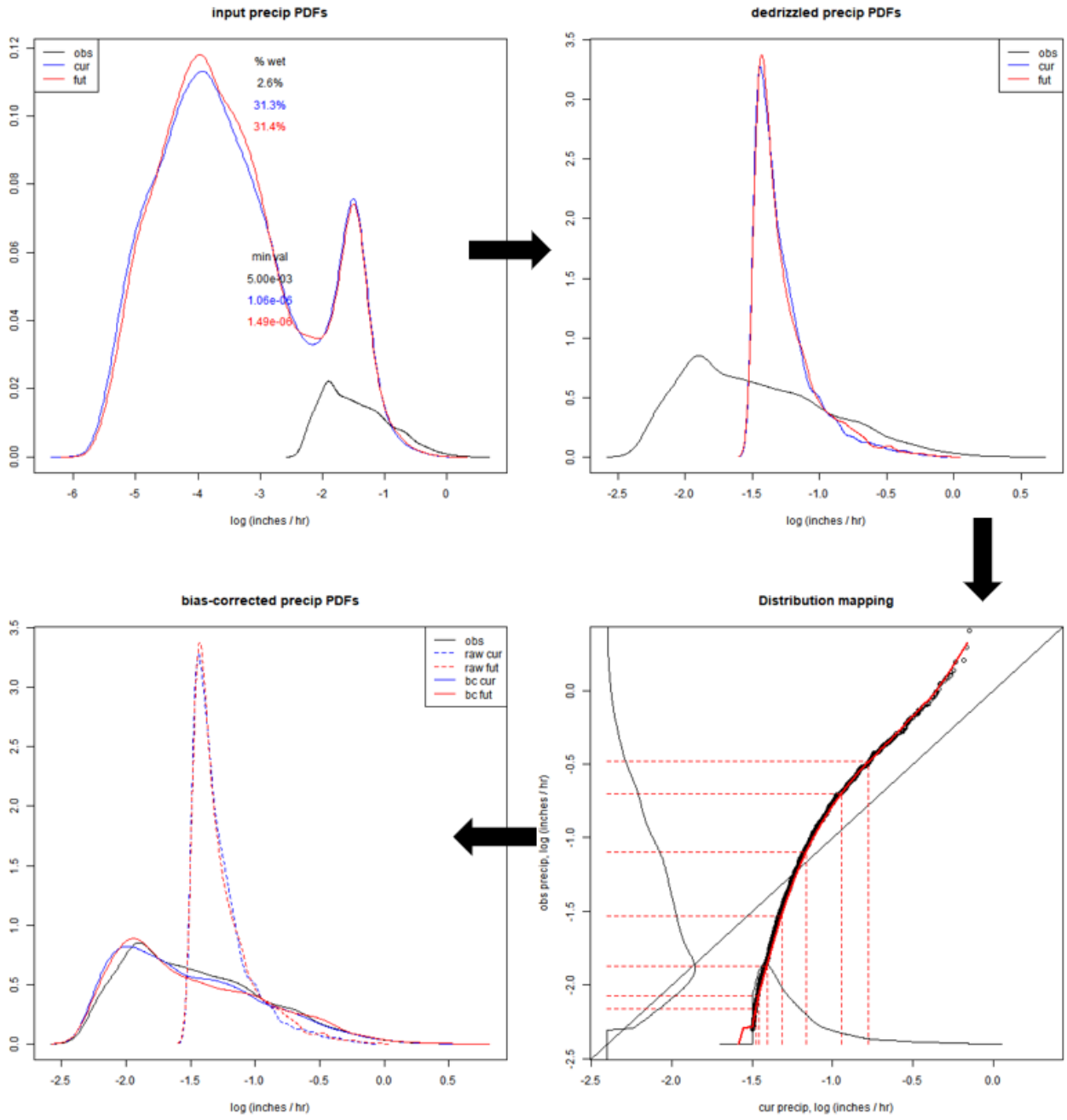

Fig. 2. KDDM bias-correction procedure steps using the R package "climod" for hourly precipitation data in Amarillo, TX, using Model 1 from Table 3

Table 5. Subcatchment design characteristics[a]

Parameter	Description	Value	Unit
Area	Area of subcatchment	1	acre
Width	Width of overland flow path for sheet flow runoff	250	ft
% Slope	Average surface slope	1	%
% Imperv	Percent impervious area	100	%
N-Imperv	Manning's n for overland flow across impervious area	0.01	-
Dstore-Imperv	Depression storage depth for impervious area	0	in
%Zero-Imperv	Percent impervious area with zero depression storage	100	%
Subarea Routing	All runoff flows directly to outlet	OUTLET	-

[a]Due to the subcatchment consisting of 100% impervious cover, all parameters solely influencing pervious cover (N-Perv, Dstore-Perv, Percent Routed, and Infiltration Data) were ignored.

Figure 3 and Table 6 provide characteristics of the bioretention cell used in the SWMM model. The surface area (5,750 ft^2) and surface layer depth (6 in) were sized to enable the bioretention cell to store the water quality storm event (Deletic 1998), which is typically the surface runoff generated from a 1-inch storm event. The soil layer is then composed of a mixture of coarse sand, topsoil, and organic matter to filter pollutants while promoting flow through high hydraulic conductivity (2 in/hr). Following flow through the soil layer, the storage layer is composed of gravel (#57 stone) with a high void ratio (0.4) to allow for water storage or seepage, (0.5 in/hr) into the native soil occurs. Lastly, to allow the storage layer to completely fill prior to draining, the bottom of the underdrain pipe is placed at the top of the storage layer (Rossman 2015).

Fig. 4 displays the SWMM model inputs used to define the process, infiltration, and routing models. The 'Rainfall/Runoff' process model was used to account for surface runoff from the subcatchment into the bioretention cell. The 'Green-Ampt' infiltration model was used for its ability to accurately represent soil infiltration using fundamental soil properties (initial soil moisture deficit, saturated hydraulic conductivity, and suction head at the wetting front) (Green and Ampt 1911). The 'Dynamic Wave' routing model was used for its accuracy above other routing models due to its ability to solve the one-dimensional Saint-Venant equations, incorporating the continuity and momentum equations (Rossman 2015). Data File inputs for the Rain Gage were observed hourly precipitation data (1999-2013) and bias-corrected future hourly precipitation data (2035-2049), each independent files. The Climatology Editor was used to input External Climate Files containing observed daily temperature data (1999-2013) and bias-corrected future daily temperature data (2035-2049).

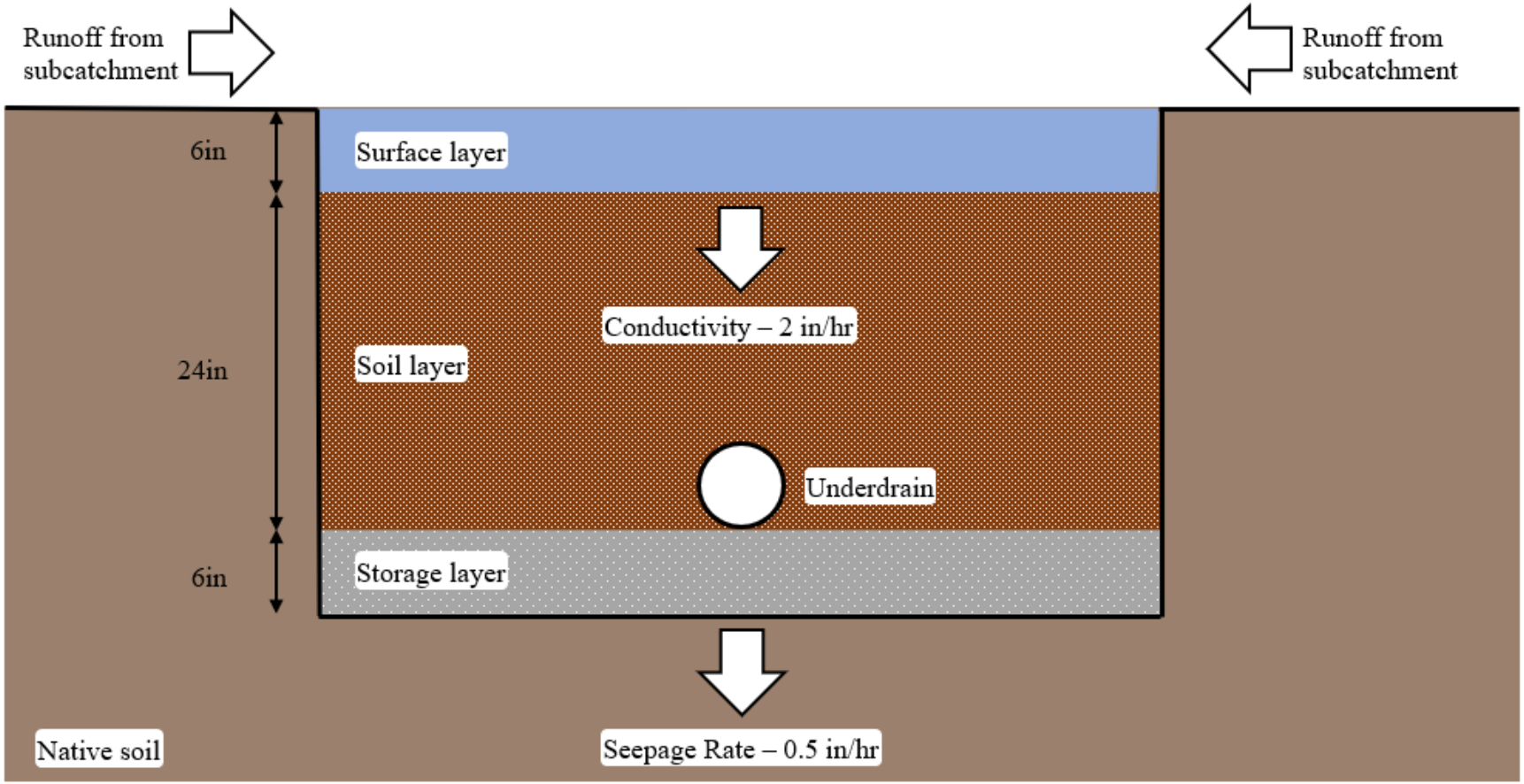

Fig. 3. Cross-sectional view of bioretention cell used in SWMM model

Table 6. Bioretention cell design characteristics

Surface Parameter	Description	Value	Unit	Source
Berm Height	Max ponding depth above surface	6	in	TDEC (2014)
Vegetation Volume Fraction	Fraction of volume filled with vegetation (ignored)	0	-	Rossman (2015)
Surface Roughness	Manning's n for overland flow (ignored)	0	-	Rossman (2015)
Surface Slope	Slope of surface (ignored)	0	%	Rossman (2015)
Soil Parameter	**Description**	**Value**	**Unit**	**Source**
Soil Thickness	Thickness of soil layer	24	in	TDEC (2014)
Porosity	Pore space volume/total soil volume	0.44	-	MSSC (2006)
Field Capacity	Pore water volume/total soil volume (following drainage)	0.09	-	MSSC (2006)
Wilting Point	Pore water volume/total soil volume (for well-dried soil)	0.04	-	MSSC (2006)
Conductivity	Hydraulic conductivity of fully saturated soil	2	in/hr	MSSC (2006)
Conductivity Slope	Slope of log(Conductivity) vs soil moisture content curve	50	-	Rossman (2015)
Suction Head	Soil capillary suction	4	in	Brakensiek et al. (1981)
Storage Parameter	**Description**	**Value**	**Unit**	**Source**
Storage Thickness	Thickness of gravel layer	6	in	County (2008)
Void Ratio	Void space volume/solid space volume	0.4	-	Miller (1978)
Seepage Rate	Rate of water seepage from storage layer into native soil	0.5	in/hr	MSSC (2006)
Clogging Factor	Clogging parameter (ignored)	0	-	Rossman (2015)
Drain Parameter	**Description**	**Value**	**Unit**	**Source**
Flow Coefficient[a] (C)	Determines drain flow rate as function of hydraulic head	0.6	-	County (2008)
Flow Exponent[a] (n)	Determines drain flow rate as function of hydraulic head	0.5	-	County (2008)
Offset	Height of drain line above bottom of storage layer	6	in	Miller (1978)

[a]Flow Coefficient and Flow Exponent are incorporated within $q = Ch^n$ where q is drain outflow rate (in/hr) and h is height of saturated media above drain (in) (Rossman 2015).

Additional details for the SWMM model may be found in the Appendix. Following completion of the SWMM model, the model was run using the observed climate data (17 scenarios) from January 1, 1999, to December 31, 2013, and the bias-corrected future climate data (170 scenarios) from January 1, 2035, to December 31, 2049. Since performance comparisons between observed and bias-corrected future climate data was the primary focus of this study, and since the model represented a hypothetical case, no calibration or model verification was performed on the SWMM model (Tirpak et al. 2021; Wang et al. 2016).

Bioretention Cell Performance Indices

The three bioretention cell performance indices compiled and assessed in this study were infiltration loss, underdrain outflow, and overflow. Infiltration loss accounts for the cumulative amount of infiltration (also referred to as seepage rate in Fig. 3 and Table 6) into the native soil beneath the storage layer. Underdrain outflow accounts for the cumulative amount of treated outflow to a receiving drainage system when the storage layer is filled and is unable to infiltrate fast enough into the native soil (TDEC 2014). Overflow accounts for the cumulative amount of surface runoff due to the bioretention cell's inability to evapotranspire, store, infiltrate, and discharge through the underdrain at a rate faster than that of the precipitation rate. Underdrain outflow and overflow should both be minimized to reduce peak runoff, treat surface runoff, and allow native soil infiltration. The three bioretention cell performance indices account for the majority of total inflow into the bioretention cell and provide quantitative measures for the efficacy of the bioretention cell.

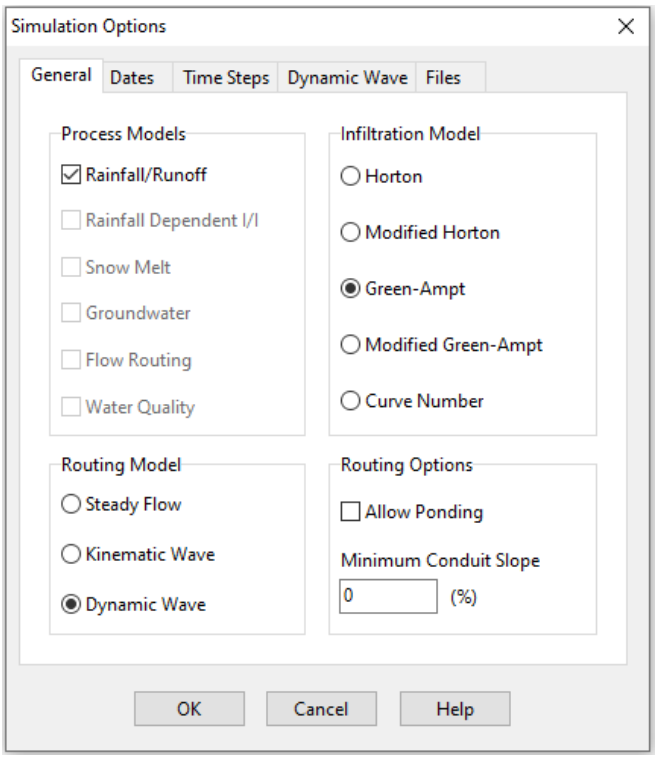

Fig. 4. SWMM Model inputs in Simulation Options

CHAPTER FOUR
RESULTS AND RECOMMENDATIONS

Results

Due to the significant number of locations (17) and models (10), climate inputs were first parsed to allow an understanding of how precipitation varied based on both the location of interest and based on which model was considered. Comparison of observed and future datasets using both categories, location and model, provides context as to how assessments of climate change effects may yield variable results based on these factors. Bioretention cell performance was then assessed using three bioretention cell performance indices: infiltration loss, underdrain outflow, and overflow.

Precipitation Statistics by Location

Table 7 provides observed (1999-2013) mean precipitation statistics for all 17 locations. Rainy days were counted as any day in either dataset in which rainfall volume was greater than 0.0 in between 00:00 and 23:59. A minimum inter-event time (MIT) of 6-hours was used to separate events in the datasets. Accordingly, aggregation was performed on any rainfall occurrence within 6-hours of a previous rainfall occurrence (e.g., 0.1in at 02:00 would be aggregated with 0.5in at 07:00 leading to a 0.6in event). The 6-hour MIT was selected due to its frequent use in literature for runoff studies (Chin et al. 2016; Guo and Adams 1998; Palynchuk and Guo 2007). While hydrologic processes such as infiltration can take longer than 6 hours, the primary use for the MIT in this study was to enable comparison between observed and future precipitation events. Therefore, any period without rainfall for 6 hours or more was accounted for in the mean drying period.

Table 7. Observed (1999-2013) mean precipitation statistics for all 17 locations

Location	Annual Rainfall (in)	Annual Rain Events	Annual Rainy Days	Drying Period (days)	Percentile Rainfall Event Depths (in)			
					50^{th}	90^{th}	99^{th}	99.9^{th}
Amarillo TX	17.8	61.3	64	5.8	0.09	0.81	2.17	4.04
Boise ID	10.2	83.1	84	4.2	0.06	0.29	0.86	1.36
Boston MA	42.2	108.7	123	3.1	0.16	1.00	2.78	6.39
Boulder CO	16.9	57.5	58	6.2	0.10	0.70	1.70	5.52
Charlotte NC	40.2	100.2	107	3.4	0.16	1.11	2.65	4.70
Chicago IL	35.9	112.2	119	3.1	0.12	0.84	2.25	6.56
El Paso TX	8.6	41.5	44	8.7	0.08	0.54	1.74	2.72
Fargo ND	22.8	90.5	95	3.9	0.08	0.65	2.22	4.31
Memphis TN	49	96.4	103	3.6	0.22	1.34	3.30	6.37
Missoula MT	12.4	115.5	116	3.0	0.04	0.27	0.86	1.89
New Orleans LA	58.6	108.5	109	3.2	0.19	1.39	5.01	10.54
Phoenix AZ	6.4	29.0	31	12.4	0.08	0.69	1.32	2.59
Pittsburgh PA	38.2	139.8	146	2.4	0.11	0.75	1.83	3.73
Portland OR	34.9	152.2	159	2.1	0.10	0.61	1.75	3.50
San Antonio TX	31.1	77.4	78	4.5	0.11	1.19	3.25	9.36
San Jose CA	11.3	42.2	43	8.5	0.12	0.70	1.60	2.86
St. Louis MO	39.9	103.7	110	3.3	0.17	1.04	2.73	4.08

Fig. 5 displays the percent change between the observed (1999-2013) and bias-corrected future (2035-2049) datasets for mean annual rainfall, mean annual rain events, mean annual rainy days, and mean drying period for the 17 locations. Percent change between the observed and future datasets was calculated using Eq. 1.

$$\%\ change = \frac{future - observed}{observed} * 100\% \quad \text{Eq. 1}$$

Each location's boxplot is composed of the percent change between the observed and future datasets for all 10 models, leading to 10 values per boxplot. Out of the 170 total future model-location combinations, annual rainfall increased in 135 combinations (79.4%); annual rain events decreased in 110 combinations (64.7%); annual rainy days decreased in 103 combinations (60.6%); and mean drying period increased in 107 combinations (62.9%). Median annual rainfall (shown in orange in Fig. 5) increased for all 17 locations while the median number of annual rain events and rainy days decreased for 9 locations with an additional 3 locations observing decreases in one of these two precipitation characteristics. Across all locations, mean annual rainfall volume increased by 9.9% (2.8in) while mean annual rain events and rainy days decreased 6.2% (6.5 days) and 3.9% (3.7 days), respectively. The greatest percent change in mean annual rainfall occurred in New Orleans with an increase of 18.7% (10.9in), while the lowest percent change occurred in Portland with an increase of 4.3% (1.5in). These trends are consistent with the understanding that while the total amount of rainfall may be higher in many locations in the future, extreme rainfall will also increase in many locations, meaning fewer events with higher magnitudes. Coupled with this anticipated reduction in the number of rainfall events, climate change is expected to bring larger drying periods between storms. Median drying period increased for 11 locations, with Portland being the only location where all 10 models projected increased annual dry days. Combining all locations, mean drying period increased by 10.5% (0.5 days) with the greatest

percent change in mean drying period occurring in New Orleans, mean increase of 37.8% (1.2 days), while no change occurred in St. Louis. Jhong and Tung (2018) showed similar results and suggested that occurrences of floods and droughts could occur more frequently due to the combination of increased precipitation event volumes and drying periods. Manka et al. (2016) also showed that increased dry periods can reduce the efficacy of the biological processes present in bioretention cells resulting in nutrient export.

Fig. 6 displays the percent change between observed (1999-2013) and future (2035-2049) precipitation volumes for 50^{th}, 90^{th}, 99^{th}, and 99.9^{th} percentile rainfall event depths for the 17 locations. This allowed a more in-depth analysis as to how event size would change under future climate projections. Out of the 170 total future model-location combinations, 50^{th} percentile events increased in 62 combinations (36.5%); 90^{th} percentile events increased in 118 combinations (69.4%); 99^{th} percentile events increased in 165 combinations (97.1%); and 99.9^{th} percentile events increased in 147 combinations (86.5%). While median 50^{th} percentile events only increased in 7 locations, upper percentile events were shown to consistently increase in size, with median 90^{th} percentile events increasing in 12 locations, median 99^{th} percentile events increasing in all 17 locations, and median 99.9^{th} percentile events increasing in 16 locations. The increased trend in upper percentile precipitation events ($\geq 90^{th}$) with minimal change in median precipitation events (50^{th}) falls in line with observations from existing literature and again points to anticipated increases in severe rainfall in the future (Karl and Knight 1998; Madsen and Figdor 2007; Olsson et al. 2009; Wang et al. 2019b). Since bioretention cells are most effective during small, lower-intensity precipitation events, the observed increase in the frequency of large, high-intensity precipitation events is particularly concerning for future bioretention cell performance (Wang et al. 2018, 2019b).

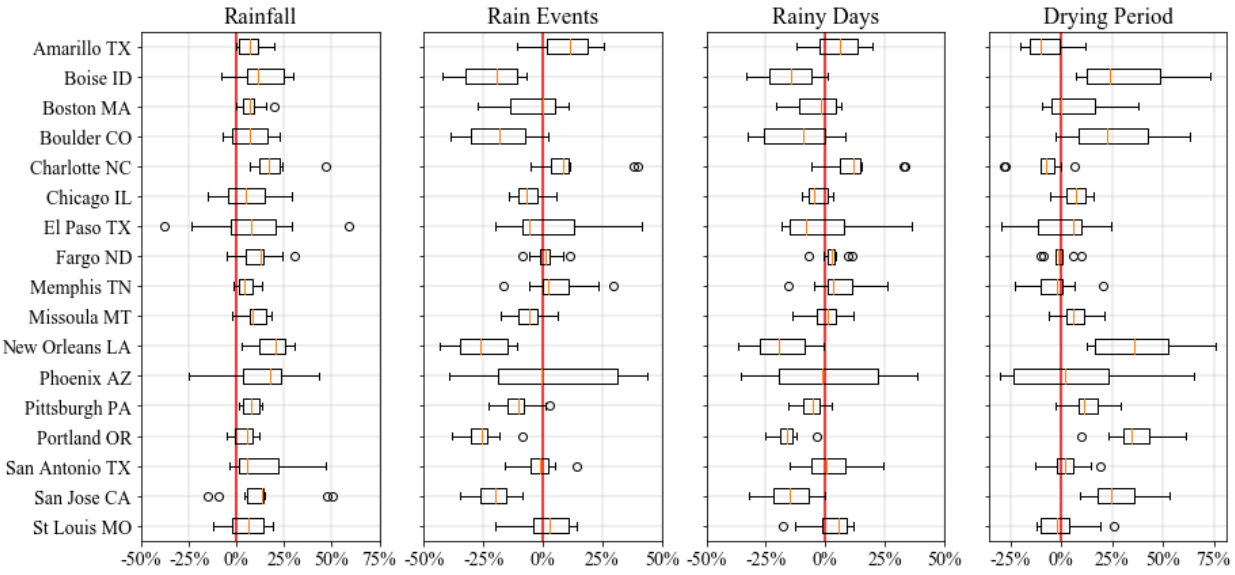

Fig. 5. Percent change between observed (1999-2013) and future (2035-2049) mean annual rainfall, mean annual rain events, mean annual rainy days, and mean drying period for the 17 locations.

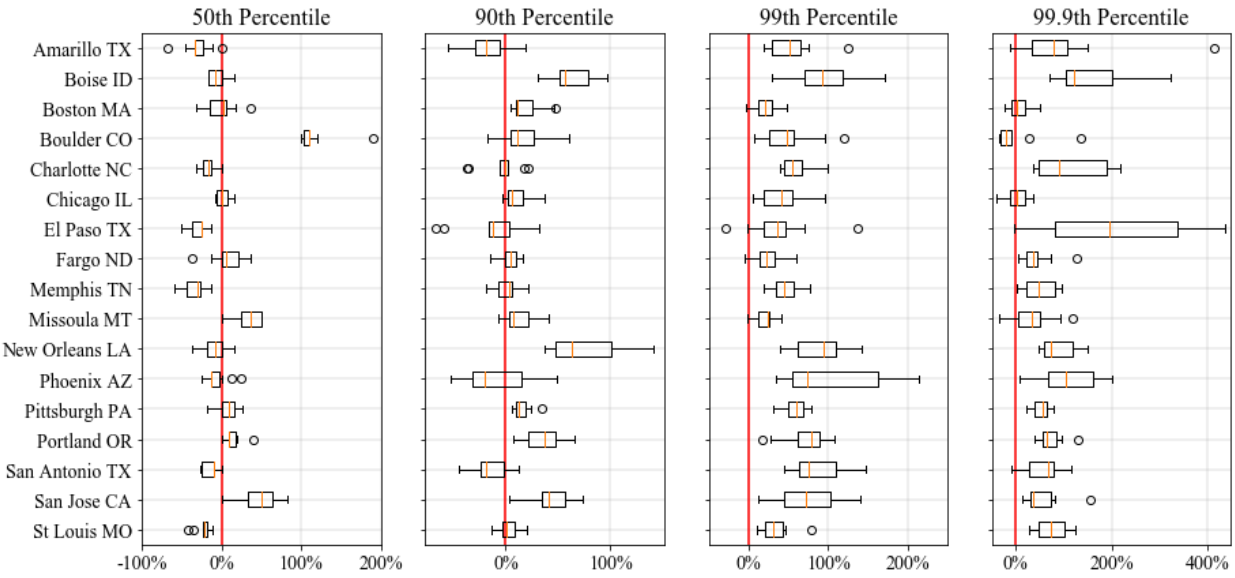

Fig. 6. Percent change between observed (1999-2013) and future (2035-2049) precipitation volumes for 50th, 90th, 99th, and 99.9th percentile rainfall event depths for the 17 locations. *Note: An extreme outlier for 99.9th percentile events in El Paso is not shown in the figure (843%).

Bioretention Cell Performance

Fig. 7 displays the percent change between the observed (1999-2013) and future (2035-2049) infiltration loss, underdrain outflow, and overflow for all 17 locations. Due to values of zero being modeled for underdrain outflow and/or overflow under the observed rainfall data, 6 boxplots are not shown for Boise, Missoula, Phoenix, Portland, and San Jose in Fig. 7 (i.e. percent change could not be calculated).

Excluding the 2 locations with increased median infiltration loss, Boise (25.9%) and Fargo (1.7%), percent change in median infiltration loss ranged from -0.2% (Portland) to -18.3% (New Orleans) in the remaining 15 locations. Conversely, excluding the 1 location with an observed underdrain outflow value of zero (Boise), percent change in median underdrain outflow increased between 9.7% (San Antonio) and 393.2% (Phoenix) in the remaining 16 locations. Finally, 5 locations had an observed overflow value of zero with the 2 outlier locations being Boulder (median decrease of 8.6%) and El Paso (median increase of 1510.4%). In the remaining 10 locations, the percent change in median overflow increased between 74.5% (Chicago) and 509.7% (Boston). The projected significant increase in overflow in 11 locations is most concerning from a public health and safety perspective due to overflow predominantly bypassing treatment and quickly proceeding to nearby conveyances (Hathaway et al. 2014; Tirpak et al. 2021).

Out of the 170 total future model-location combinations, overflow increased in 151 combinations (88.8%); underdrain outflow increased in 163 combinations (95.9%); and infiltration loss decreased in 121 combinations (71.2%). The increase in overflow and underdrain outflow combined with decreased infiltration loss indicate bioretention cells designed with existing guidelines may be unable to accommodate the projected increase in upper percentile storm magnitudes; specifically, surface infiltration may not be fast enough to avoid significant increases in overflow. The decrease in infiltration loss is both a consequence and cause of this detrimental

feedback loop. Increased annual precipitation volume and intensity expedite the rainfall-runoff process and increase runoff, thereby reducing infiltration and increasing overflow. Thus, the primary benefits of bioretention cells (e.g., reducing peak runoff, groundwater recharge, filtering pollutants) may be lessened under future climate change scenarios.

Decreased infiltration loss under increased rainfall volumes has been documented in literature before (Tirpak et al. 2021), but the root cause has not been investigated. The root cause of this relationship is most likely due to either the bioretention cell's surface layer filling too quickly, disallowing surface infiltration (and subsequent infiltration loss) due to immediate surface runoff, or infiltration loss being driven primarily by the number of rain events. If the surface layer is filling too quickly to enable surface infiltration, then the surface layer depth could be increased to hold a greater runoff volume, providing additional time for surface infiltration to occur. However, if infiltration loss is driven primarily by the number of rain events (e.g., minimal change in infiltration loss regardless of event size), then decreased infiltration loss may be inevitable under future climate scenarios projecting decreased rain events.

Fig. 8 displays the percent change between the observed (1999-2013) and future (2035-2049) mean yearly overflow days, 50^{th} percentile daily overflow, 90^{th} percentile daily overflow, and 99^{th} percentile daily overflow. Due to observed values of zero for overflow, Boise, Missoula, Phoenix, Portland, and San Jose are not shown in Fig. 8 (i.e. percent change could not be calculated). Percent change in median yearly overflow days increased between 14.8% (New Orleans) and 334.6% (El Paso) for all 12 locations shown. The percent increase in median yearly overflow days and the associated variability between locations is highly related to the increase in extreme precipitation events. Winston (2016) found similar variability in future precipitation when comparing locations only 15.5 miles apart in northeast Ohio. Similarly, Gao et al. (2012) showed

substantial variability in climate change effects on extreme weather across the eastern United States.

Of the 12 locations shown in Fig. 8, 6 locations (Boston, Boulder, Chicago, El Paso, New Orleans, and Pittsburgh) also decreased in median number of annual rainy days, again indicating increases in rainfall magnitude when events do occur. A particularly compelling example of this trend is found in New Orleans, where a relatively low increase in median yearly overflow days in New Orleans is found, yet the location shows a significant increase in median annual precipitation (18.7%) and decrease in median annual rainy days (19.5%) – the largest percent changes in both precipitation statistics – suggesting larger events will make up a larger percentage of the storms that do occur.

Excluding Boulder and Chicago, median 50^{th}, 90^{th}, and 99^{th} percentile daily overflow increased for the 10 remaining locations shown in Fig. 8. Excluding the western and northwestern United States, the consistent increase across all overflow percentiles indicates that government agencies, city planners, and stormwater engineers should expect higher overflow volumes for all events to become the new standard across the United States. Boston, Charlotte, Memphis, and New Orleans face the greatest likelihood of higher overflow volumes. All 4 locations experienced ≥100% increases for all three (50^{th}, 90^{th}, and 99^{th}) median daily overflow percentiles with all 10 models projecting increases. The increase across all overflow percentiles and models indicates that the size of overflow volumes will not only possibly escalate, but this change is statistically likely to occur in those 4 locations. Therefore, stormwater professionals for those 4 locations will need to begin modifying existing bioretention cells to ensure they are capable of maintaining their existing function into the future.

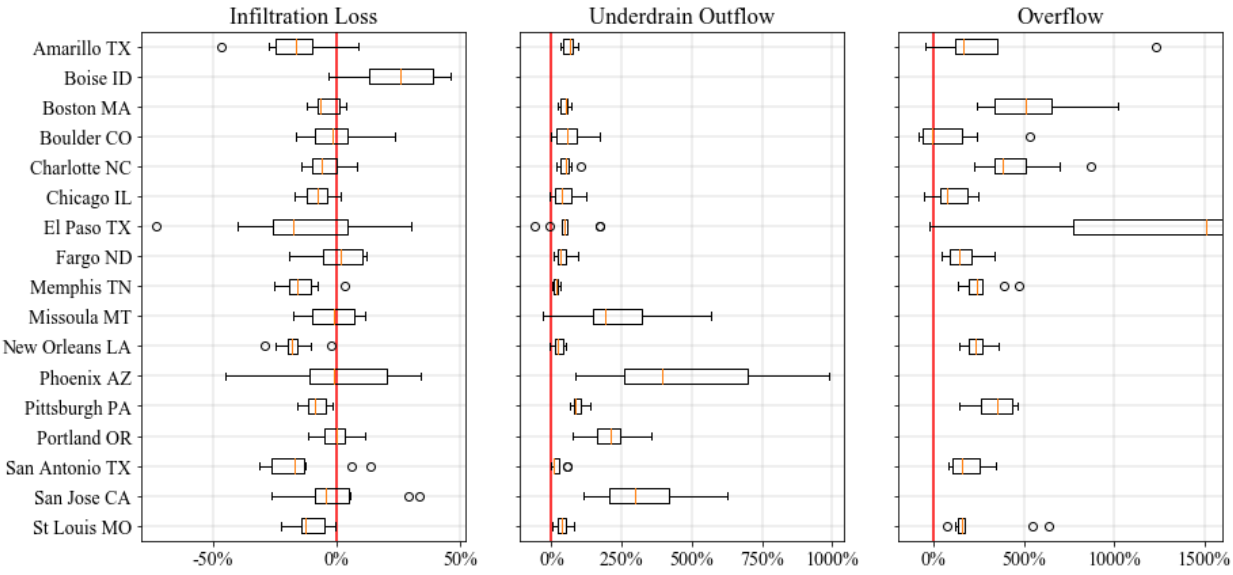

Fig. 7. Percent change between observed (1999-2013) and bias-corrected future (2035-2049) bioretention cell performance indices, infiltration loss, underdrain outflow, and overflow for 17 locations.
*Note: Second half of boxplot for El Paso is cut off from the figure (Q_3 = 2487%; Max = 5360%).

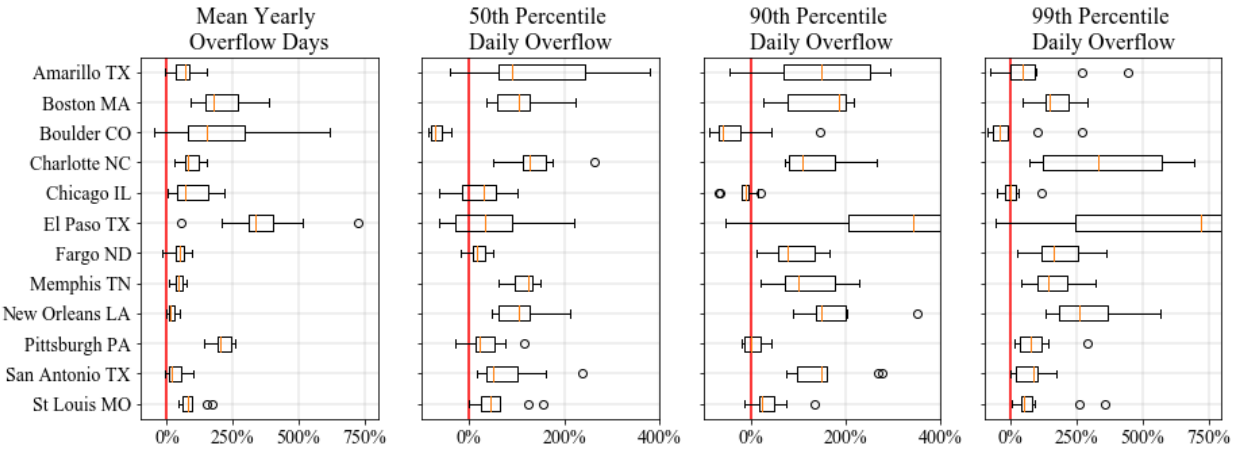

Fig. 8. Percent change between observed (1999-2013) and bias-corrected future (2035-2049) overflow characteristics for 12 locations.
*Note: An outlier for Amarillo is cut off from the 90th percentile figure (Max = 766%), and the second half of the boxplot for El Paso is cut off from the 90th percentile figure (Q_3 = 689%; Max = 1147%) and 99th percentile figure (Q_3=1211%; Max = 4353%).

Fig. 9 provides comparison of observed (1999-2013) and future (2035-2049) median overflow, underdrain outflow, and infiltration loss results for all 17 locations. The sum of all three bioretention cell performance indices (overflow, underdrain outflow, and infiltration loss) is hereafter referred to as "annual volume". Median overflow increased in 15 locations, remained unchanged in 1 location (Boise), and decreased in 1 location (Boulder); underdrain outflow increased in all 17 locations; and infiltration loss decreased in all 17 locations. Due to many locations having extremely low overflow or underdrain outflow under the observed precipitation dataset, relative comparisons between observed and future datasets have been made using changes in the percent of total annual volume attributed to each hydrologic pathway as opposed to using percent change (e.g., comparing 1% with 5% instead of stating a 400% increase). Relative percent change between the observed and future datasets was calculated using Eq. 2.

$$relative\ \%\ change = future\ \% - observed\ \% \qquad \text{Eq. 2}$$

Bioretention cells in the southern United States are most at risk of being unable to provide their existing function under future climate change scenarios. The 7 southern-most locations (Amarillo, Charlotte, El Paso, Memphis, New Orleans, Phoenix, and San Antonio) produced all 7 of the highest relative percent increases in overflow, ranging from 7.0% to 19.6%. With the exception of Memphis, the 7 southern-most locations also produced 6 of the highest relative percent decreases in infiltration loss, ranging from 15.3% to 24.0%. New Orleans and San Antonio also recorded the two highest relative median increases in overflow, 2766.5 cu yd/yr and 928.6 cu yd/yr, respectively. Significant increases in overflow in the southern and southwestern United States are consistent with extreme precipitation projections by Prein et al. (2017) and bioretention cell performance analysis literature (Cook et al. 2019; Hathaway et al. 2014). The significant increases in overflow are a direct result of the frequent and intense rainfall in the southern United States,

which will only further exacerbate existing stormwater infrastructure and cause more flooding. Although GSI is likely to provide some resiliency to extreme precipitation, these results indicate there are limits in this resilience that can be exceeded.

While not under the same degree of risk as the southern United States, bioretention cells located in the Midwest and Northeast are still at risk of losing their existing function under future climate change scenarios. Following the 7 southern locations, the 5 locations in the Midwest and Northeast (Boston, Chicago, Fargo, Pittsburgh, and St. Louis) produced the next 5 highest relative percent increases in overflow, ranging from 3.3% to 5.2%. The 5 Midwest and Northeast locations also recorded the 5th through 9th highest relative median increases in overflow, ranging from 230.5 cu yd/yr to 315.4 cu yd/yr. Results are consistent with Cook et al. (2019) who found that bioretention cells in the Midwest and Northeast overflowed equivalent or elevated magnitudes of runoff compared to other regions in the United States.

Bioretention cells in the western and northwestern United States have the best likelihood of being able to maintain their existing function under future climate change scenarios. The 5 northwestern-most locations (Boise, Boulder, Missoula, Portland, and San Jose) produced all 5 of the lowest relative percent changes in overflow, ranging from a decrease of 0.3% to an increase of 1.2%. The 5 northwestern-most locations also recorded all 5 of the lowest relative changes in overflow, ranging from a median decrease of 5.5 cu yd/yr to an increase of 28.1 cu yd/yr. With the exception of Boulder, the extremely positive bioretention cell performances in the northwest are consistent with results from Cook et al. (2019). The minimal effect on existing bioretention cell function indicates that stormwater infrastructure in the northwestern United States will require the least additional investment under climate change scenarios to maintain existing function.

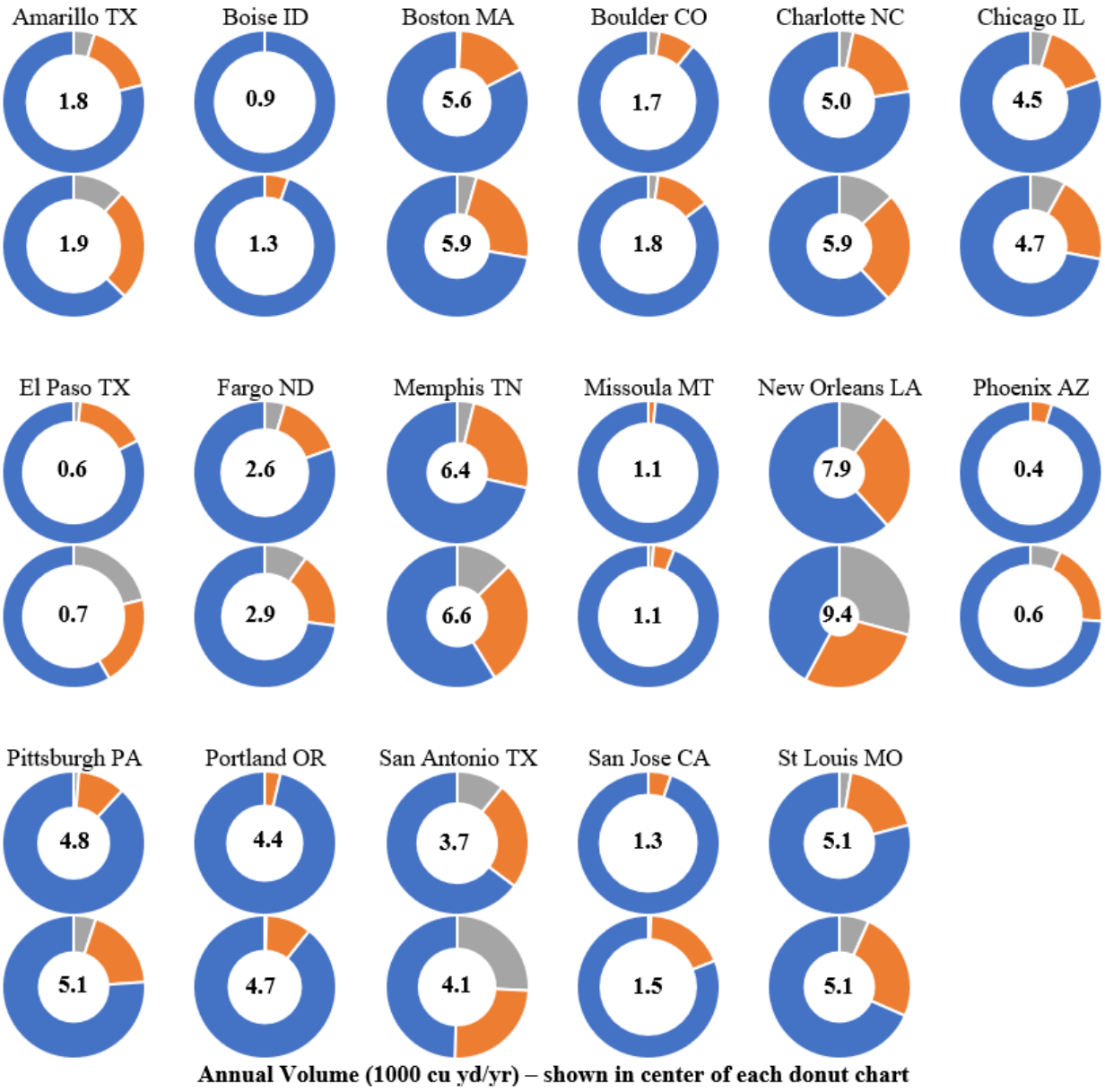

Fig. 9. Observed (top) and future (bottom) overflow (grey), underdrain outflow (orange), and infiltration loss (blue) for all 17 locations. Donut hole size is inversely proportional to the annual volume.

Recommendations

While many bioretention cells across the United States are projected to experience significant increases in overflow and decreases in infiltration, modifications can be performed to mitigate the effects of climate change.

Management Strategies

Tirpak et al. (2021) compared an ensemble of retrofit and design configurations for bioretention cells in east Tennessee, and found varying degrees of success for three scenarios: 1) increasing the soil layer depth; 2) increasing the storage layer depth; 3) and increasing the bioretention cell surface area. Increasing the depth of the soil layer in the bioretention cell was shown to be a conservative yet effective method of increasing runoff volume retention (Tirpak et al. 2021). As such, increasing the depth of the soil layer for bioretention cells in regions where overflow is expected to increase some but not significantly, such as the western and northwestern United States and parts of the Midwest, is a viable option requiring low investment. Increased soil layer depth can also increase pollutant removal and water storage (Hatt et al. 2009; Muerdter et al. 2016; Read et al. 2008). Vegetation in bioretention cells of the western and northwestern United States would benefit greatly from the increased water storage due to the projected significant decrease in rainy days and increase in drying period.

Increasing the depth of the storage layer has been found to be an extremely effective method of reducing overflow. Hathaway et al. (2014) found an increased storage layer depth of 3.6 to 12.4 inches would maintain existing function in east North Carolina into the late 2050's, and Winston (2016) found an increased storage layer depth of 2 to 6.8 inches would maintain existing function in northeast Ohio into the late 2050's. Increased storage layer depth has the potential to store a greater volume of runoff than increased soil layer depth but requires either deepening the

bioretention cell or removing media from the soil layer, reducing the efficacy of pollutant removal. However, increasing the storage layer depth is more effective at reducing overflow than increasing the soil layer depth and should be considered if overflow reduction is the priority (Tirpak et al. 2021). Densely populated, highly urbanized locations with a future need for additional overflow volume retention, such as Chicago, Pittsburgh, or Boston, would greatly benefit from increased storage layer depths in bioretention cells.

The final successful option investigated by Tirpak et al. (2021) increased the surface area of bioretention cells while keeping the subcatchment area constant, which has been shown to be an effective method of reducing overflow and increasing infiltration (Wang et al. 2019a, 2019b). Increasing bioretention cell surface area has the greatest potential for reducing overflow and increasing infiltration if all other bioretention cell characteristics are held constant. Essentially, this in turn causes soil and storage layer volumes to increase, improving overall storage capacity. Soil and storage layer depths can also be increased while increasing surface area, adding additional storage volume. Increasing the bioretention cell's surface area requires the greatest investment of the three options and may not be an option in some locations due to urbanization or cost. However, locations in the southern United States, El Paso, San Antonio, Memphis, Charlotte, and New Orleans, will require significant investment in all stormwater infrastructure (grey and green) to eliminate or at least reduce overflow volumes. A location such as New Orleans, in particular, will need to incorporate bioretention cell modifications wherever possible to reduce the significant increases in projected overflow volumes.

CHAPTER FIVE
CONCLUSION

The increased frequency and severity of extreme precipitation events caused by climate change pose significant risk to urban stormwater infrastructure. Although bioretention cells are considered to be a way to build resiliency into drainage systems, their performance under climate change is largely untested. This study investigated the performance of bioretention cells under future climate scenarios across the contiguous United States. Future simulated climate data from 17 locations and 10 RCMs (170 total combinations) were gathered and bias-corrected using the kernel density distribution mapping technique. Bioretention cell simulations were then performed in EPA SWMM 5.1 using bias-corrected future (2035-2049) and observed (1999-2013) climate data to enable performance comparisons.

Median annual rainfall increased across all 17 locations in future scenarios. A majority of locations also experienced a decreased median number of rainy days and rain events while median drying period increased. Precipitation events were projected to become significantly more severe for upper-percentile events ($\geq 90^{th}$) while 50^{th} percentile events were projected to change minimally for all locations except for Boulder. Extreme upper-percentile events increased the most consistently across locations with 17 locations increasing in 99^{th} percentile events and 16 locations increasing in 99.9^{th} percentile events. Future precipitation events will, therefore, become less frequent but more severe. The combination of increased precipitation event severity and volume with increased drying period also indicates floods and droughts will occur more frequently in the future. However, findings clearly indicate that while precipitation event severity is expected to increase on average across the United States the shift in precipitation patterns will vary significantly by location.

As a result of shifting precipitation patterns, future bioretention cell performance changed across all locations. Relative percent increases in annual underdrain outflow and/or overflow and decreases in annual infiltration loss occurred for all 17 locations. Increased annual overflow poses significant environmental and health risks to urban communities due to the runoff bypassing treatment, amplifying downstream flows, and potentially transporting pollutants, pathogens, and sediment. Percent increases in median 50^{th}, 90^{th}, and 99^{th} percentile overflow events are also projected for 10 locations. Excluding the western and northwestern United States, higher overflow volumes for all event percentiles should be expected across the United States. Decreased infiltration presents an additional challenge for city planners and stormwater engineers. If bioretention cells are no longer able to promote native soil infiltration and filter pollutants, then their benefit as a stormwater control measure will be lost. Further, these outcomes suggest that while bioretention buffers extreme weather, there are limitations in this buffering capacity during large events.

Findings show that the future performance of bioretention cells built under current guidelines will vary significantly by region. The southern United States is projected to experience the most significant shift in precipitation patterns with bioretention cells very likely losing their existing function if unchanged. However, recent research suggests significant investment in retrofits or design modifications of existing bioretention cells in the southern United States have the potential to heavily minimize the effects of climate change. The Midwest and Northeast are projected to experience a less severe shift in precipitation patterns compared to the southern United States, but bioretention cells are still likely to lose their existing function if unchanged. Moderate investments in retrofits or design modifications in the Midwest and Northeast could enable bioretention cells to maintain or even improve their existing function in the future. The western

and northwestern United States have the best projected future outlook compared to all other regions. Minor investments in retrofits or design modifications of bioretention cells in the western and northwestern United States would ensure existing or improved function regardless of the future model scenario.

Future studies should be performed incorporating a wider range of climate models, emissions scenarios, and bioretention cell configurations. The range of climate models and emissions scenarios used in this study was limited based on the availability of simulated hourly precipitation data. Only two emissions scenarios were used in this study with 1 model based on RCP4.5 and 9 models based on RCP8.5. As such, additional climate models used for each emissions scenario would further elucidate trends in future climate. While a range of climate models and locations were evaluated in this study, a single bioretention cell configuration was used for all simulations. A future study incorporating this methodology with multiple bioretention cell configurations would provide insight on the significance of design modifications required in all locations to maintain existing function under future climate scenarios.

LIST OF REFERENCES

Ahiablame, L. M., B. A. Engel and I. Chaubey. 2012. "Effectiveness of Low Impact Development Practices: Literature Review and Suggestions for Future Research." *Water Air Soil Pollut.* 223(7): 4253-4273. https://doi.org/10.1007/s11270-012-1189-2.

Ahiablame, L. and R. Shakya. 2016. "Modeling flood reduction effects of low impact development at a watershed scale." *J. Environ. Manage.* 171: 81-91. https://doi.org/10.1016/j.jenvman.2016.01.036.

Arcement, G. J. and V. R. Schneider. 1989. "Guide for selecting Manning's roughness coefficients for natural channels and flood plains." US Geology Survey, Denver, CO.

Arguez, A., S. Hurley, A. Inamdar, L. Mahoney, A. Sanchez-Lugo and L. Yang. 2020. "Should We Expect Each Year in the Next Decade (2019–28) to Be Ranked among the Top 10 Warmest Years Globally?" *Bull. Am. Meteorol. Soc.* 101(5): E655-E663. https://doi.org/10.1175/BAMS-D-19-0215.1.

Ault, T. R., J. E. Cole, J. T. Overpeck, G. T. Pederson and D. M. Meko. 2014. "Assessing the Risk of Persistent Drought Using Climate Model Simulations and Paleoclimate Data." *J. Clim.* 27(20): 7529-7549. https://doi.org/10.1175/JCLI-D-12-00282.1.

Berg, P., C. Moseley and J. O. Haerter. 2013. "Strong increase in convective precipitation in response to higher temperatures." *Nat. Geosci.* 6(3): 181-185. https://doi.org/10.1038/ngeo1731.

Berggren, K., M. Olofsson, M. Viklander, G. Svensson and A.-M. Gustafsson. 2012. "Hydraulic impacts on urban drainage systems due to changes in rainfall caused by climatic change." *J. Hydrol. Eng.* 17(1): 92-98. https://doi.org/10.1061/(ASCE)HE.1943-5584.0000406.

Bhaduri, B., J. Harbor, B. Engel and M. Grove. 2000. "Assessing Watershed-Scale, Long-Term Hydrologic Impacts of Land-Use Change Using a GIS-NPS Model." *Environ. Manage.* 26(6): 643-658. https://doi.org/10.1007/s002670010122.

Bhaduri, B., M. Minner, S. Tatalovich and J. Harbor. 2001. "Long-Term Hydrologic Impact of Urbanization: A Tale of Two Models." *J. Water Resour. Plan. Manag.* 127(1): 13-19. https://doi.org/10.1061/(ASCE)0733-9496(2001)127:1(13).

Biglarbeigi, P., W. A. Strong, D. Finlay, R. McDermott and P. Griffiths. 2020. "A Hybrid Model-Based Adaptive Framework for the Analysis of Climate Change Impact on Reservoir Performance." *Water Resour. Manag.* 34(13): 4053-4066. https://doi.org/10.1007/s11269-020-02654-w.

Bishop, D. A., A. P. Williams and R. Seager. 2019. "Increased Fall Precipitation in the Southeastern United States Driven by Higher-Intensity, Frontal Precipitation." *Geophys. Res. Lett.* 46(14): 8300-8309. https://doi.org/10.1029/2019GL083177.

Bonneau, J., T. D. Fletcher, J. F. Costelloe, P. J. Poelsma, R. B. James and M. J. Burns. 2020. "The hydrologic, water quality and flow regime performance of a bioretention basin in Melbourne, Australia." *Urban Water J.* 17(4): 303-314. https://doi.org/10.1080/1573062X.2020.1769688.

Bounoua, L., P. Zhang, G. Mostovoy, K. Thome, J. Masek, M. Imhoff, M. Shepherd, D. Quattrochi, J. Santanello, J. Silva, R. Wolfe and A. M. Toure. 2015. "Impact of urbanization on US surface climate." *Environ. Res. Lett.* 10(8): 084010. https://doi.org/10.1088/1748-9326/10/8/084010.

Brakensiek, D. L., R. L. Engleman and W. J. Rawls. 1981. "Variation within Texture Classes of Soil Water Parameters." Transactions of the ASAE 24(2): 0335-0339. https://dx.doi.org/10.13031/2013.34253.

Bukovsky, M. S. 2011. "Masks for the Bukovsky regionalization of North America." Regional Integrated Sciences Collective, Institute for Mathematics Applied to Geosciences, National Center for Atmospheric Research. Accessed March 2, 2021. http://www.narccap.ucar.edu/contrib/bukovsky/.

Bukovsky, M. S., J. A. Thompson and L. O. Mearns. 2019. "Weighting a regional climate model ensemble: Does it make a difference? Can it make a difference?" *Clim. Res.* 77(1): 23-43. https://doi.org/10.3354/cr01541.

Bukovsky, M. S. and L. O. Mearns. 2020. "Regional climate change projections from NA-CORDEX and their relation to climate sensitivity." *Clim. Change* 162(2): 645-665. https://doi.org/10.1007/s10584-020-02835-x.

Chan, F. K. S., J. A. Griffiths, D. Higgitt, S. Xu, F. Zhu, Y.-T. Tang, Y. Xu and C. R. Thorne. 2018. "“Sponge City” in China—A breakthrough of planning and flood risk management in the urban context." *Land Use Policy* 76: 772-778. https://dx.doi.org/10.1016/j.landusepol.2018.03.005.

Chapman, C. and R. R. Horner. 2010. "Performance Assessment of a Street-Drainage Bioretention System." *Water Environ. Res.* 82(2): 109-119. https://dx.doi.org/10.2175/106143009x426112.

Chen, J., L. Theller, M. W. Gitau, B. A. Engel and J. M. Harbor. 2017. "Urbanization impacts on surface runoff of the contiguous United States." *J. Environ. Manage.* 187: 470-481. https://doi.org/10.1016/j.jenvman.2016.11.017.

Chin, R. J., S. H. Lai, K. B. Chang, W. Z. W. Jaafar and F. Othman. 2016. "Relationship between minimum inter-event time and the number of rainfall events in Peninsular Malaysia." *Weather* 71(9): 213-218. https://doi.org/10.1002/wea.2766.

Cook, L. M. 2018. "Using climate change projections to increase the resilience of stormwater infrastructure designs under uncertainty. " Doctoral dissertation, Pittsburgh, PA: Carnegie Mellon Univ.

Cook, L. M., J. M. VanBriesen and C. Samaras. 2019. "Using rainfall measures to evaluate hydrologic performance of green infrastructure systems under climate change." *Sustainable Resilient Infrastruct.* 1-25. https://doi.org/10.1080/23789689.2019.1681819.

Cook, L. M., S. McGinnis and C. Samaras. 2020. "The effect of modeling choices on updating intensity-duration-frequency curves and stormwater infrastructure designs for climate change." *Clim. Change* 159(2): 289-308. https://doi.org/10.1007/s10584-019-02649-6.

County, K. 2008. "Knox County Tennessee stormwater management manual." Compiled by AMEC Earth & Environmental Inc, Knoxville, TN.

Davis, A. P. 2008. "Field Performance of Bioretention: Hydrology Impacts." *J. Hydrol. Eng.* 13(2): 90-95. https://doi.org/10.1061/(ASCE)1084-0699(2008)13:2(90).

Davis, A. P., M. Shokouhian, H. Sharma and C. Minami. 2001. "Laboratory Study of Biological Retention for Urban Stormwater Management." *Water Environ. Res.* 73(1): 5-14. https://doi.org/10.2175/106143001X138624.

Davis, A. P., M. Shokouhian, H. Sharma, C. Minami and D. Winogradoff. 2003. "Water Quality Improvement through Bioretention: Lead, Copper, and Zinc Removal." *Water Environ. Res.* 75(1): 73-82. https://doi.org/10.2175/106143003X140854.

Davis, A. P., M. Shokouhian, H. Sharma and C. Minami. 2006. "Water Quality Improvement through Bioretention Media: Nitrogen and Phosphorus Removal." *Water Environ. Res.* 78(3): 284-293. https://doi.org/10.2175/106143005X94376.

Deletic, A. 1998. "The first flush load of urban surface runoff." *Water Res.* 32(8): 2462-2470. https://doi.org/10.1016/S0043-1354(97)00470-3.

Denault, C., R. G. Millar and B. J. Lence. 2006. "Assessment of possible impacts of climate change in an urban catchment." *J. Am. Water Resour. Assoc.* 42(3): 685-697. https://doi.org/10.1111/j.1752-1688.2006.tb04485.x.

Dietz, M. E. 2007. "Low Impact Development Practices: A Review of Current Research and Recommendations for Future Directions." *Water Air Soil Pollut.* 186(1-4): 351-363. https://doi.org/10.1007/s11270-007-9484-z.

Dietz, M. E. and J. C. Clausen. 2005. "A Field Evaluation of Rain Garden Flow and Pollutant Treatment." *Water Air Soil Pollut.* 167(1-4): 123-138. https://doi.org/10.1007/s11270-005-8266-8.

Dietz, M. E. and J. C. Clausen. 2008. "Stormwater runoff and export changes with development in a traditional and low impact subdivision." *J. Environ. Manage.* 87(4): 560-566. https://doi.org/10.1016/j.jenvman.2007.03.026.

Donat, M. G., A. L. Lowry, L. V. Alexander, P. A. O'Gorman and N. Maher. 2016. "More extreme precipitation in the world's dry and wet regions." *Nat. Clim Change* 6(5): 508-513. https://doi.org/10.1038/nclimate2941.

Du, J., L. Qian, H. Rui, T. Zuo, D. Zheng, Y. Xu and C. Y. Xu. 2012. "Assessing the effects of urbanization on annual runoff and flood events using an integrated hydrological modeling system for Qinhuai River basin, China." *J. Hydrol.* 464-465: 127-139. https://doi.org/10.1016/j.jhydrol.2012.06.057.

Dupont, B. and D. L. Allen. 1999. "Revision of the Rainfall-intensity Duration Curves for the commonwealth of Kentucky."

Eckart, K., Z. McPhee and T. Bolisetti. 2017. "Performance and implementation of low impact development – A review." *Sci. Total Environ.* 607-608: 413-432. https://dx.doi.org/10.1016/j.scitotenv.2017.06.254.

Ezber, Y., O. Lutfi Sen, T. Kindap and M. Karaca. 2007. "Climatic effects of urbanization in istanbul: a statistical and modeling analysis." *Int. J. Climatol.* 27(5): 667-679. https://doi.org/10.1002/joc.1420.

Fischer, E. M. and R. Knutti. 2016. "Observed heavy precipitation increase confirms theory and early models." *Nat. Clim. Change* 6(11): 986-991. https://doi.org/10.1038/nclimate3110.

Gao, Y., J. S. Fu, J. B. Drake, Y. Liu and J. F. Lamarque. 2012. "Projected changes of extreme weather events in the eastern United States based on a high resolution climate modeling system." *Environ. Res. Lett.* 7(4): 044025. https://dx.doi.org/10.1088/1748-9326/7/4/044025.

Garschagen, M. and P. Romero-Lankao. 2015. "Exploring the relationships between urbanization trends and climate change vulnerability." *Clim. Change* 133(1): 37-52. https://doi.org/10.1007/s10584-013-0812-6.

Gill, S. E., J. F. Handley, A. R. Ennos and S. Pauleit. 2007. "Adapting cities for climate change: the role of the green infrastructure." *Built Environ.* 33(1): 115-133. https://doi.org/10.2148/benv.33.1.115.

Gironás, J., L. A. Roesner, and J. Davis. 2009. "Storm Water Management Model Applications Manual". US Environmental Protection Agency, EPA: Washington, DC, US.

Green, W. H. and G. A. Ampt. 1911. "Studies on Soil Phyics." *J. Agric. Sci.* 4(1): 1-24. https://dx.doi.org/10.1017/s0021859600001441.

Groisman, P. Y., R. W. Knight, D. R. Easterling, T. R. Karl, G. C. Hegerl and V. N. Razuvaev. 2005. "Trends in Intense Precipitation in the Climate Record." *J. Clim.* 18(9): 1326-1350. https://dx.doi.org/10.1175/jcli3339.1.

Gunn, R., A. Martin, B. Engel and L. Ahiablame. 2012. "Development of two indices for determining hydrologic implications of land use changes in urban areas." *Urban Water J.* 9(4): 239-248. https://dx.doi.org/10.1080/1573062x.2012.660957.

Guo, Y. and B. J. Adams. 1998. "Hydrologic analysis of urban catchments with event-based probabilistic models: 1. Runoff volume." *Water Resour. Res.* 34(12): 3421-3431. https://doi.org/10.1029/98WR02449.

Hamill, T. M. 2014. "Performance of Operational Model Precipitation Forecast Guidance during the 2013 Colorado Front-Range Floods." *Mon. Weather Rev.* 142(8): 2609-2618. https://dx.doi.org/10.1175/mwr-d-14-00007.1.

Hargreaves, G. H. and Z. A. Samani. 1985. "Reference Crop Evapotranspiration from Temperature." *Appl. Eng. Agric.* 1(2): 96-99. https://doi.org/10.13031/2013.26773.

Hathaway, J. M., R. A. Brown, J. S. Fu and W. F. Hunt. 2014. "Bioretention function under climate change scenarios in North Carolina, USA." *J. Hydrol.* 519: 503-511. https://doi.org/10.1016/j.jhydrol.2014.07.037.

Hatt, B. E., T. D. Fletcher and A. Deletic. 2009. "Hydrologic and pollutant removal performance of stormwater biofiltration systems at the field scale." *J. Hydrol.* 365(3): 310-321. https://doi.org/10.1016/j.jhydrol.2008.12.001.

Horton, R., C. Rosenzweig, V. Gornitz, D. Bader and M. O'Grady. 2010. "CLIMATE RISK INFORMATION." *Ann. N. Y. Acad. Sci.* 1196(1): 147-228. https://doi.org/10.1111/j.1749-6632.2010.05323.x.

Huong, H. T. L. and A. Pathirana. 2013. "Urbanization and climate change impacts on future urban flooding in Can Tho city, Vietnam." *Hydrol. Earth Syst. Sci.* 17(1): 379-394. https://doi.org/10.5194/hess-17-379-2013.

IPCC. 2013. "What is a GCM?" Accessed March 2, 2021. https://www.ipcc-data.org/guidelines/pages/gcm_guide.html.

Ivancic, T. J. and S. B. Shaw. 2016. "A U.S.-based analysis of the ability of the Clausius-Clapeyron relationship to explain changes in extreme rainfall with changing temperature." *J. Geophys. Res. Atmos.* 121(7): 3066-3078. https://doi.org/10.1002/2015JD024288.

Jhong, B.-C. and C.-P. Tung. 2018. "Evaluating Future Joint Probability of Precipitation Extremes with a Copula-Based Assessing Approach in Climate Change." *Water Resour. Manag.* 32(13): 4253-4274. https://doi.org/10.1007/s11269-018-2045-y.

Kalnay, E. and M. Cai. 2003. "Impact of urbanization and land-use change on climate." *Nature* 423(6939): 528-531. https://doi.org/10.1038/nature01675.

Karl, T. R. and R. W. Knight. 1998. "Secular Trends of Precipitation Amount, Frequency, and Intensity in the United States." *Bull. Am. Meteorol. Soc.* 79(2): 231-241. https://dx.doi.org/10.1175/1520-0477(1998)079<0231:stopaf>2.0.co;2.

Kaufmann, R. K., H. Kauppi, M. L. Mann and J. H. Stock. 2011. "Reconciling anthropogenic climate change with observed temperature 1998-2008." *Proc. Natl. Acad. Sci.* 108(29): 11790-11793. https://dx.doi.org/10.1073/pnas.1102467108.

Kendon, E. J., N. M. Roberts, H. J. Fowler, M. J. Roberts, S. C. Chan and C. A. Senior. 2014. "Heavier summer downpours with climate change revealed by weather forecast resolution model." *Nat. Clim Change* 4(7): 570-576. https://doi.org/10.1038/nclimate2258.

Kirtman, B., S. B. Power, A. J. Adedoyin, G. J. Boer, R. Bojariu, I. Camilloni, F. Doblas-Reyes, A. M. Fiore, M. Kimoto, and G. Meehl. 2013. Near-term climate change: projections and predictability. Cambridge University Press, Cambridge, United Kingdom and New York, NY, USA, 953–1028.

Köppen, W. 1900. Versuch einer Klassifikation der Klimate, Vorzugsweise nach ihren Beziehungen zur Pflanzenwelt [Attempted climate classification in relation to plant distributions]. [In German]. *Geogr. Z.*, 6, 593-611, 657-679.

Kuo, C.-C., T. Y. Gan and M. Gizaw. 2015. "Potential impact of climate change on intensity duration frequency curves of central Alberta." *Clim. Change* 130(2): 115-129. https://doi.org/10.1007/s10584-015-1347-9.

Lanzante, J. R., D. Adams-Smith, K. W. Dixon, M. Nath and C. E. Whitlock. 2020. "Evaluation of some distributional downscaling methods as applied to daily maximum temperature with emphasis on extremes." *Int. J. Climatol.* 40(3): 1571-1585. https://doi.org/10.1002/joc.6288.

Lenderink, G. and E. van Meijgaard. 2010. "Linking increases in hourly precipitation extremes to atmospheric temperature and moisture changes." *Environ. Res. Lett.* 5(2): 025208. http://dx.doi.org/10.1088/1748-9326/5/2/025208.

Leopold, L. B. 1968. Hydrology for urban land planning: A guidebook on the hydrologic effects of urban land use, US Geological Survey.

Line, D. E. and W. F. Hunt. 2009. "Performance of a Bioretention Area and a Level Spreader-Grass Filter Strip at Two Highway Sites in North Carolina." *J. Irrig. Drain. Eng.* 135(2): 217-224. https://doi.org/10.1061/(ASCE)0733-9437(2009)135:2(217).

Lucas, W. C. and D. J. Sample. 2015. "Reducing combined sewer overflows by using outlet controls for Green Stormwater Infrastructure: Case study in Richmond, Virginia." *J. Hydrol.* 520: 473-488. https://doi.org/10.1016/j.jhydrol.2014.10.029.

Luell, S. K., W. F. Hunt and R. J. Winston. 2011. "Evaluation of undersized bioretention stormwater control measures for treatment of highway bridge deck runoff." *Water Sci. Technol.* 64(4): 974-979. https://dx.doi.org/10.2166/wst.2011.736.

Madsen, T. and E. Figdor. 2007. When it rains, it pours: global warming and the rising frequency of extreme precipitation in the US. Environment America Research and Policy Center. Boston.

Mahmoud, S. H. and T. Y. Gan. 2018. "Urbanization and climate change implications in flood risk management: Developing an efficient decision support system for flood susceptibility mapping." *Sci. Total Environ.* 636: 152-167. https://doi.org/10.1016/j.scitotenv.2018.04.282.

Mailhot, A., S. Duchesne, D. Caya and G. Talbot. 2007. "Assessment of future change in intensity–duration–frequency (IDF) curves for Southern Quebec using the Canadian Regional Climate Model (CRCM)." *J. Hydrol.* 347(1-2): 197-210. https://doi.org/10.1016/j.jhydrol.2007.09.019.

Manka, B. N., J. M. Hathaway, R. A. Tirpak, Q. He and W. F. Hunt. 2016. "Driving forces of effluent nutrient variability in field scale bioretention." *Ecol. Eng.* 94: 622-628. https://doi.org/10.1016/j.ecoleng.2016.06.024.

Masson-Delmotte, V., P. Zhai, H.-O. Pörtner, D. Roberts, J. Skea, P.R. Shukla, A. Pirani, W. Moufouma-Okia, C. Péan, R. Pidcock, S. Connors, J.B.R. Matthews, Y. Chen, X. Zhou, M.I. Gomis, E. Lonnoy, T. Maycock, M. Tignor, and T. Waterfield. 2018. Global Warming of 1.5°C. An IPCC Special Report on the impacts of global warming of 1.5°C above pre-industrial levels and related global greenhouse gas emission pathways, in the context of strengthening the global response to the threat of climate change, sustainable development, and efforts to eradicate poverty, IPCC.

McGinnis, S. 2018. "climod: Bias correction and other tools for climate model output. Version 0.0.1." Accessed March 10, 2021. https://github.com/sethmcg/climod.

McGinnis, S., D. Nychka and L. O. Mearns. 2015. A new distribution mapping technique for climate model bias correction. *Machine learning and data mining approaches to climate science*, Springer: 91-99.

McGinnis, S. A. and L. Mearns. 2016. "Bias-Correction of Extreme Temperatures and Precipitation in NA-CORDEX Regional Climate Model Output." AGUFM 2016: GC53B-1290.

Mearns et al. 2017. "The NA-CORDEX dataset, version 1.0." NCAR Climate Data Gateway. Accessed March 2, 2021. https://doi.org/10.5065/D6SJ1JCH.

Meehl, G. A., F. Zwiers, J. Evans, T. Knutson, L. Mearns and P. Whetton. 2000. "Trends in Extreme Weather and Climate Events: Issues Related to Modeling Extremes in Projections of Future Climate Change*." *Bull. Am. Meteorol. Soc.* 81(3): 427-436. https://dx.doi.org/10.1175/1520-0477(2000)081<0427:tiewac>2.3.co;2.

Mei, C., J. Liu, H. Wang, Z. Yang, X. Ding and W. Shao. 2018. "Integrated assessments of green infrastructure for flood mitigation to support robust decision-making for sponge city construction in an urbanized watershed." *Sci. Total Environ.* 639: 1394-1407. https://dx.doi.org/10.1016/j.scitotenv.2018.05.199.

Miller, R. 1978. The hydraulically effective impervious area of an urban basin, Broward County, Florida. Prepared for the International Symposium on Urban Storm Water Management, Kentucky University, Lexington, July 24-27, 1978.

Milly, P., J. Betancourt, M. Falkenmark, R. M. Hirsch, Z. W. Kundzewicz, D. P. Lettenmaier and R. J. Stouffer 2008. "Stationarity is dead: Whither water management?" *Earth* 4: 20.

Minnesota Stormwater Steering Committee (MSSC). 2006. Minnesota Stormwater Manual. Minnesota Pollution Control Agency, St. Paul, MN.

Moore, T. L., J. S. Gulliver, L. Stack and M. H. Simpson. 2016. "Stormwater management and climate change: vulnerability and capacity for adaptation in urban and suburban contexts." *Clim. Change* 138(3-4): 491-504. https://doi.org/10.1007/s10584-016-1766-2.

Muerdter, C., E. Özkök, L. Li and A. P. Davis. 2016. "Vegetation and Media Characteristics of an Effective Bioretention Cell." *J. Sustain. Water Built Environ.* 2(1): 04015008. https://doi.org/10.1061/JSWBAY.0000804.

Nelson, K. C. and M. A. Palmer. 2007. "Stream Temperature Surges Under Urbanization and Climate Change: Data, Models, and Responses1." *J. Am. Water Resour. Assoc* 43(2): 440-452. https://doi.org/10.1111/j.1752-1688.2007.00034.x.

Nelson, K. C., M. A. Palmer, J. E. Pizzuto, G. E. Moglen, P. L. Angermeier, R. H. Hilderbrand, M. Dettinger and K. Hayhoe. 2009. "Forecasting the combined effects of urbanization and climate change on stream ecosystems: from impacts to management options." *J. Appl. Ecol.* 46(1): 154-163. https://doi.org/10.1111/j.1365-2664.2008.01599.x.

National Oceanic and Atmospheric Administration (NOAA). 2016. National Centers for Environmental Information. Accessed June 1, 2020. https://www.ncdc.noaa.gov/.

National Oceanic and Atmospheric Administration (NOAA). 2017. National Weather Service. Accessed January 20, 2021. https://hdsc.nws.noaa.gov/hdsc/pfds/.

O'Driscoll, M., S. Clinton, A. Jefferson, A. Manda and S. McMillan. 2010. "Urbanization Effects on Watershed Hydrology and In-Stream Processes in the Southern United States." *Water* 2(3): 605-648. https://dx.doi.org/10.3390/w2030605.

Oleson, K. W., G. B. Anderson, B. Jones, S. A. McGinnis and B. Sanderson. 2018. "Avoided climate impacts of urban and rural heat and cold waves over the U.S. using large climate model ensembles for RCP8.5 and RCP4.5." *Clim. Change* 146(3): 377-392. https://doi.org/10.1007/s10584-015-1504-1.

Olsson, J., K. Berggren, M. Olofsson and M. Viklander. 2009. "Applying climate model precipitation scenarios for urban hydrological assessment: A case study in Kalmar City, Sweden." *Atmos. Res.* 92(3): 364-375. https://doi.org/10.1016/j.atmosres.2009.01.015.

Pachauri, R. K., M. R. Allen, V. R. Barros, J. Broome, W. Cramer, R. Christ, … and J. P. van Ypserle. 2014. Climate change 2014: synthesis report. Contribution of Working Groups I, II and III to the fifth assessment report of the Intergovernmental Panel on Climate Change. Geneva, Switzerland, IPCC.

Palynchuk, B. and Y. Guo. 2008. "Threshold analysis of rainstorm depth and duration statistics at Toronto, Canada." *J. Hydrol.* 348(3-4): 535-545. https://doi.org/10.1016/j.jhydrol.2007.10.023.

Panofsky, H. A. and G. W. Brier. 1968. *Some applications of statistics to meteorology*. University Park, PA: Pennsylvania State University Press.

Perry, T. and R. Nawaz. 2008. "An investigation into the extent and impacts of hard surfacing of domestic gardens in an area of Leeds, United Kingdom." *Lands. Urban Plan.* 86(1): 1-13. https://doi.org/10.1016/j.landurbplan.2007.12.004.

Pielke, R. A., G. Marland, R. A. Betts, T. N. Chase, J. L. Eastman, J. O. Niles, D. D. S. Niyogi and S. W. Running. 2002. "The influence of land-use change and landscape dynamics on the climate system: relevance to climate-change policy beyond the radiative effect of greenhouse gases." *Philos. Trans. R. Soc. A* 360(1797): 1705-1719. https://dx.doi.org/10.1098/rsta.2002.1027.

Prein, A. F., R. M. Rasmussen, K. Ikeda, C. Liu, M. P. Clark and G. J. Holland. 2017. "The future intensification of hourly precipitation extremes." *Nat. Clim Change* 7(1): 48-52. https://doi.org/10.1038/nclimate3168.

Prudhomme, C., I. Giuntoli, E. L. Robinson, D. B. Clark, N. W. Arnell, R. Dankers, B. M. Fekete, W. Franssen, D. Gerten, S. N. Gosling, S. Hagemann, D. M. Hannah, H. Kim, Y. Masaki, Y. Satoh, T. Stacke, Y. Wada and D. Wisser. 2014. "Hydrological droughts in the 21st century, hotspots and uncertainties from a global multimodel ensemble experiment." *Proc. Natl. Acad. Sci* 111(9): 3262-3267. https://doi.org/10.1073/pnas.1222473110.

Pryor, S. C., J. A. Howe and K. E. Kunkel. 2009. "How spatially coherent and statistically robust are temporal changes in extreme precipitation in the contiguous USA?" *Int. J. Climatol.* 29(1): 31-45. https://dx.doi.org/10.1002/joc.1696.

R Core Team. 2020. "R: A language and environment for statistical computing. " R Foundation for Statistical Computing, Vienna, Austria. Accessed March 10, 2020. http://www.r-project.org/index.html.

Read, J., T. Wevill, T. Fletcher and A. Deletic. 2008. "Variation among plant species in pollutant removal from stormwater in biofiltration systems." *Water Res.* 42(4): 893-902. https://doi.org/10.1016/j.watres.2007.08.036.

Rosenzweig, C., D. Karoly, M. Vicarelli, P. Neofotis, Q. Wu, G. Casassa, A. Menzel, T. L. Root, N. Estrella, B. Seguin, P. Tryjanowski, C. Liu, S. Rawlins and A. Imeson. 2008. "Attributing physical and biological impacts to anthropogenic climate change." *Nature* 453(7193): 353-357. https://doi.org/10.1038/nature06937.

Rossman, L. 2015. "Storm Water Management Model User's Manual Version 5.1—Manual." US EPA Office of Research and Development, EPA: Washington, DC, USA.

Roy, A. H., M. C. Freeman, B. J. Freeman, S. J. Wenger, W. E. Ensign and J. L. Meyer. 2005. "Investigating hydrologic alteration as a mechanism of fish assemblage shifts in urbanizing streams." *J. N. Am. Benthol. Soc.* 24(3): 656-678. https://doi.org/10.1899/04-022.1.

Schlea, D., J. F. Martin, A. D. Ward, L. C. Brown and S. A. Suter. 2014. "Performance and Water Table Responses of Retrofit Rain Gardens." *J. Hydrol. Eng.* 19(8): 05014002. https://dx.doi.org/10.1061/(asce)he.1943-5584.0000797.

Schroeer, K. and G. Kirchengast. 2018. "Sensitivity of extreme precipitation to temperature: the variability of scaling factors from a regional to local perspective." *Clim. Dyn.* 50(11): 3981-3994. https://doi.org/10.1007/s00382-017-3857-9.

Schueler, T. R., L. Fraley-McNeal and K. Cappiella. 2009. "Is Impervious Cover Still Important? Review of Recent Research." *J. Hydrol. Eng.* 14(4): 309-315. https://doi.org/10.1061/(ASCE)1084-0699(2009)14:4(309).

Semadeni-Davies, A., C. Hernebring, G. Svensson and L.-G. Gustafsson. 2008. "The impacts of climate change and urbanisation on drainage in Helsingborg, Sweden: Suburban stormwater." *J. Hydrol.* 350(1): 114-125. https://doi.org/10.1016/j.jhydrol.2007.11.006.

Sennikovs, J. and U. Bethers. 2009. Statistical downscaling method of regional climate model results for hydrological modelling. 18th World IMACS Congress and MODSIM09 International Congress on Modelling and Simulation, edited by: Anderssen, RS, Braddock, RD, and Newham, LTH, Citeseer.

Sheather, S. J. 2004. "Density estimation." *Stat. Sci*. 588-597.

Shuster, W. D., J. Bonta, H. Thurston, E. Warnemuende and D. R. Smith. 2005. "Impacts of impervious surface on watershed hydrology: A review." *Urban Water J.* 2(4): 263-275. https://doi.org/10.1080/15730620500386529.

Solaiman, T. A. S., and S. P. Simonovic. 2011. Development of Probability Based Intensity-Duration-Frequency Curves under Climate Change. WATER RESOURCES RESEARCH REPORT. London, Ontario, Canada, Western University. 34.

Stephens, G. L., T. L'Ecuyer, R. Forbes, A. Gettelmen, J. C. Golaz, A. Bodas-Salcedo, K. Suzuki, P. Gabriel and J. Haynes. 2010. "Dreary state of precipitation in global models." *J. Geophys. Res. Atmos.* 115(D24). https://doi.org/10.1029/2010JD014532.

Suriya, S. and B. V. Mudgal. 2012. "Impact of urbanization on flooding: The Thirusoolam sub watershed – A case study." *J. Hydrol.* 412-413: 210-219. https://doi.org/10.1016/j.jhydrol.2011.05.008.

Tang, Z., B. A. Engel, B. C. Pijanowski and K. J. Lim. 2005. "Forecasting land use change and its environmental impact at a watershed scale." *J. Environ. Manage.* 76(1): 35-45. https://dx.doi.org/10.1016/j.jenvman.2005.01.006.

Tennessee Department of Environment and Conservation (TDEC). 2014. Tennessee Permanent Stormwater Management and Design Guidance Manual. Tennessee Department of Environment and Conservation, Division of Water Resources, Nashville, TN.

Teutschbein, C. and J. Seibert. 2012. "Bias correction of regional climate model simulations for hydrological climate-change impact studies: Review and evaluation of different methods." *J. Hydrol.* 456-457: 12-29. https://doi.org/10.1016/j.jhydrol.2012.05.052.

Thornthwaite, C.W. 1984. An approach toward a rational classification of climate. *Geogr. Rev.*, 38, 55-94. https://doi.org/10.2307/210739.

Tirpak, A., J. M. Hathaway, A. Khojandi, M. Weathers, and T. H. Epps. 2021. "Building Resiliency to Climate Change Uncertainty through Bioretention Design Modifications." *J. Environ. Manage.* 287: 112300. https://doi.org/10.1016/j.jenvman.2021.112300.

Tong, S. T. Y. and W. Chen. 2002. "Modeling the relationship between land use and surface water quality." *J. Environ. Manage.* 66(4): 377-393. https://dx.doi.org/10.1006/jema.2002.0593.

Trenberth, K. E., A. Dai, R. M. Rasmussen and D. B. Parsons. 2003. "The Changing Character of Precipitation." *Bull. Am. Meteorol. Soc.* 84(9): 1205-1218. https://doi.org/10.1175/BAMS-84-9-1205.

United Nations. 2018. *2018 Revision of world urbanization prospects*, Department of Economic and Social Affairs of the United Nations, Washington, D.C.

Utsumi, N., S. Seto, S. Kanae, E. E. Maeda and T. Oki. 2011. "Does higher surface temperature intensify extreme precipitation?" *Geophys. Res. Lett.* 38(16). https://doi.org/10.1029/2011GL048426.

Walsh, C. J., A. H. Roy, J. W. Feminella, P. D. Cottingham, P. M. Groffman and R. P. Morgan. 2005. "The urban stream syndrome: current knowledge and the search for a cure." *J. N. Am. Benthol. Soc.* 24(3): 706-723. https://dx.doi.org/10.1899/04-028.1.

Walsh, C. J., T. D. Fletcher and M. J. Burns. 2012. "Urban Stormwater Runoff: A New Class of Environmental Flow Problem." *PLOS ONE* 7(9): e45814. https://doi.org/10.1371/journal.pone.0045814.

Wang, M., D. Zhang, A. Adhityan, W. J. Ng, J. Dong and S. K. Tan. 2016. "Assessing cost-effectiveness of bioretention on stormwater in response to climate change and urbanization for future scenarios." *J. Hydrol.* 543: 423-432. https://dx.doi.org/10.1016/j.jhydrol.2016.10.019.

Wang, G., D. Wang, K. E. Trenberth, A. Erfanian, M. Yu, Michael G. Bosilovich and D. T. Parr. 2017a. "The peak structure and future changes of the relationships between extreme precipitation and temperature." *Nat. Clim Change* 7(4): 268-274. https://doi.org/10.1038/nclimate3239.

Wang, M., D. Q. Zhang, J. Su, A. P. Trzcinski, J. W. Dong and S. K. Tan. 2017b. "Future Scenarios Modeling of Urban Stormwater Management Response to Impacts of Climate Change and Urbanization." *Clean* 45(10): 1700111. https://doi.org/10.1002/clen.201700111.

Wang, M., D. Q. Zhang, J. Su, J. W. Dong and S. K. Tan. 2018. "Assessing hydrological effects and performance of low impact development practices based on future scenarios modeling." *J. Clean. Prod.* 179: 12-23. https://doi.org/10.1016/j.jclepro.2018.01.096.

Wang, M., D. Zhang, S. Lou, Q. Hou, Y. Liu, Y. Cheng, J. Qi and S. K. Tan. 2019a. "Assessing hydrological effects of bioretention cells for urban stormwater runoff in response to climatic changes." *Water* 11(5): 997. https://doi.org/10.3390/w11050997.

Wang, M., D. Zhang, Y. Cheng and S. K. Tan. 2019b. "Assessing performance of porous pavements and bioretention cells for stormwater management in response to probable climatic changes." *J. Environ. Manage.* 243: 157-167. https://doi.org/10.1016/j.jenvman.2019.05.012.

Westra, S., H. Fowler, J. Evans, L. Alexander, P. Berg, F. Johnson, E. Kendon, G. Lenderink and N. Roberts. 2014. "Future changes to the intensity and frequency of short-duration extreme rainfall." *Rev. Geophys.* 52(3): 522-555. https://doi.org/10.1002/2014RG000464.

Winston, R. J. 2016. "Resilience of Green Infrastructure under Extreme Conditions." Doctoral dissertation, Raleigh, NC: North Carolina State Univ.

Winston, R. J., J. D. Dorsey and W. F. Hunt. 2016. "Quantifying volume reduction and peak flow mitigation for three bioretention cells in clay soils in northeast Ohio." *Sci. Total Environ.* 553: 83-95. https://doi.org/10.1016/j.scitotenv.2016.02.081.

Zhang, H.-M., B. Huang, J. Lawrimore, M. Menne, and T. M. Smith. 2018a. "NOAA Global Surface Temperature Dataset (NOAAGlobalTemp), Version 4.0." NOAA National Centers for Environmental Information. Accessed January 20, 2021. doi:10.7289/V5FN144H.

Zhang, W., G. Villarini, G. A. Vecchi and J. A. Smith. 2018b. "Urbanization exacerbated the rainfall and flooding caused by hurricane Harvey in Houston." *Nature* 563(7731): 384-388. https://doi.org/10.1038/s41586-018-0676-z.

Zhang, K., D. Manuelpillai, B. Raut, A. Deletic and P. M. Bach. 2019. "Evaluating the reliability of stormwater treatment systems under various future climate conditions." *J. Hydrol.* 568: 57-66. https://doi.org/10.1016/j.jhydrol.2018.10.056.

APPENDIX

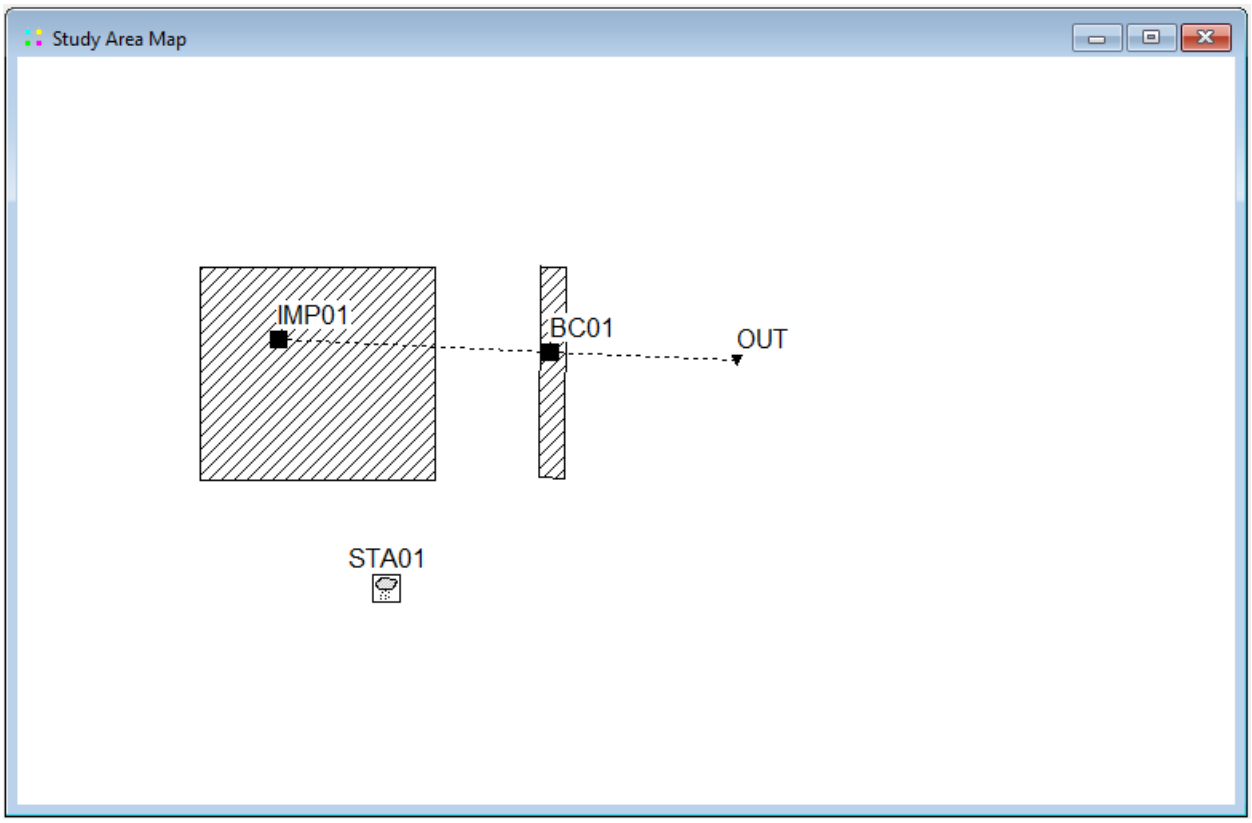

Fig. A1. SWMM model overview, including subcatchment (IMP01), bioretention cell (BC01), rain gage (STA01), and outlet (OUT)

Rain Gage STA01

Property	Value
Name	STA01
X-Coordinate	916.955
Y-Coordinate	7670.127
Description	
Tag	
Rain Format	VOLUME
Time Interval	1:00
Snow Catch Factor	1.0
Data Source	FILE
TIME SERIES:	
- Series Name	*
DATA FILE:	
- File Name	C:\Users\mweath\Desktop\United States\SWMM v2\Future\RCP45_CanESM2_CanRCM4_NAM-44\Amarillo TX\fut_precip_RCP45_CanESM2_CanRCM4_NAM-44.dat
- Station ID	STA01
- Rain Units	IN

User-assigned name of rain gage

Fig. A2. SWMM model rain gage (STA01) characteristics

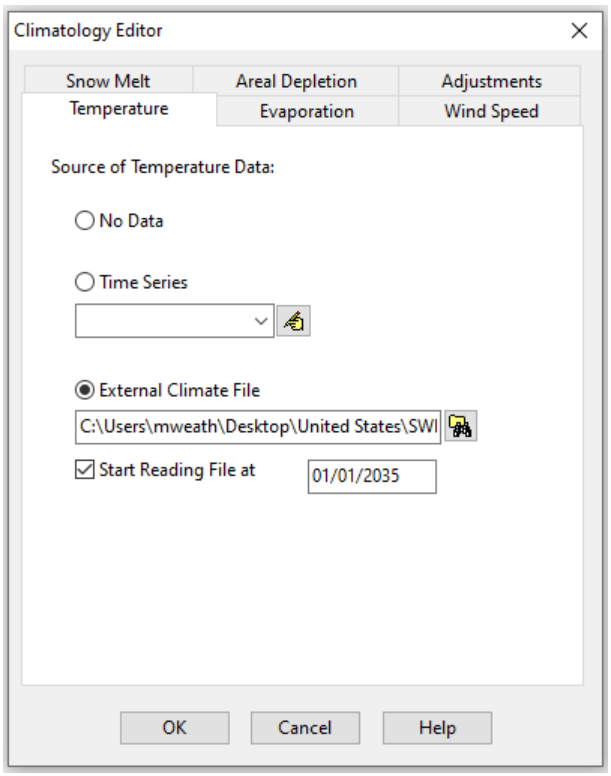

Fig. A3. SWMM model Climatology Editor Temperature tab

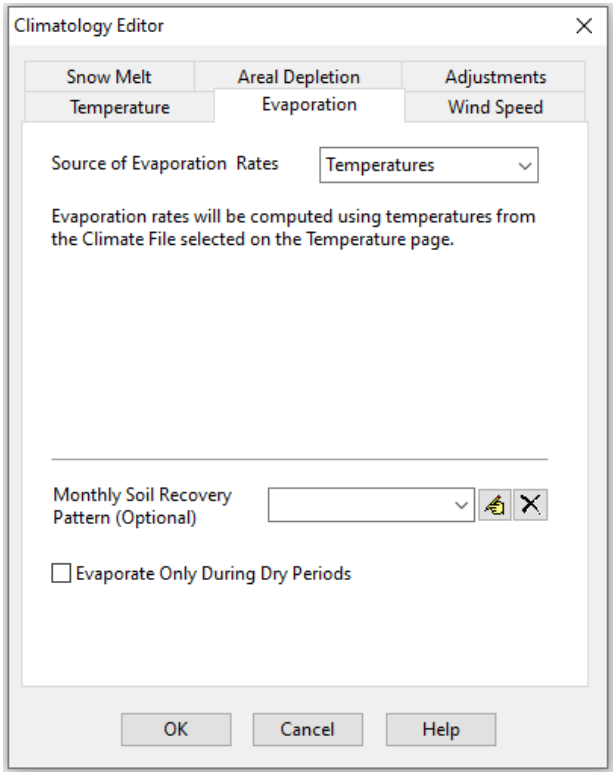

Fig. A4. SWMM model Climatology Editor Evaporation tab

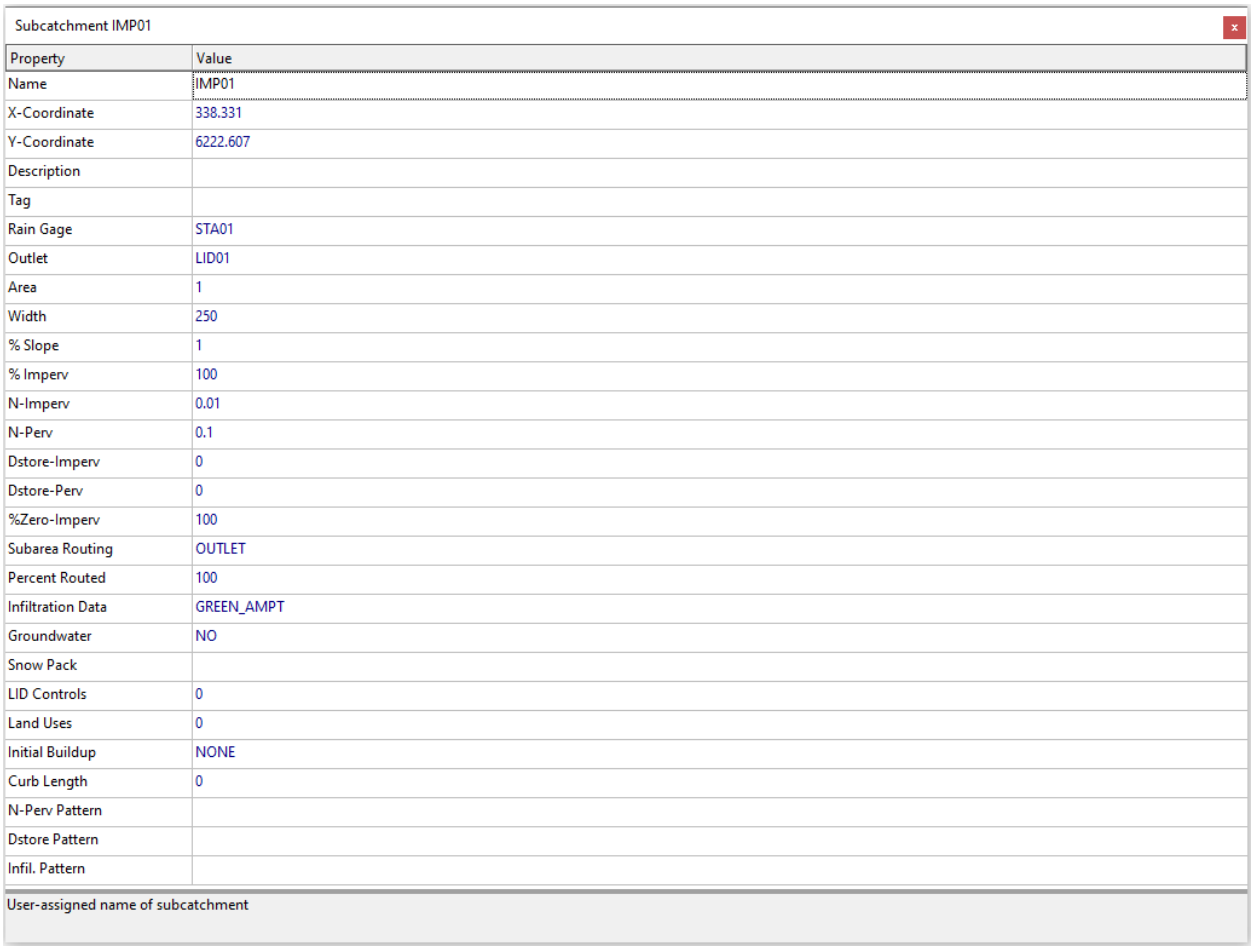

Fig. A5. SWMM model subcatchment (IMP01) characteristics

Subcatchment BC01

Property	Value
Name	BC01
X-Coordinate	3978.599
Y-Coordinate	6070.039
Description	
Tag	
Rain Gage	STA01
Outlet	OUT
Area	.132
Width	300
% Slope	1
% Imperv	0
N-Imperv	0.1
N-Perv	0.1
Dstore-Imperv	0
Dstore-Perv	0
%Zero-Imperv	100
Subarea Routing	OUTLET
Percent Routed	100
Infiltration Data	GREEN_AMPT
Groundwater	NO
Snow Pack	
LID Controls	1
Land Uses	0
Initial Buildup	NONE
Curb Length	0
N-Perv Pattern	
Dstore Pattern	
Infil. Pattern	

User-assigned name of subcatchment

Fig. A6. SWMM model bioretention cell (BC01) characteristics

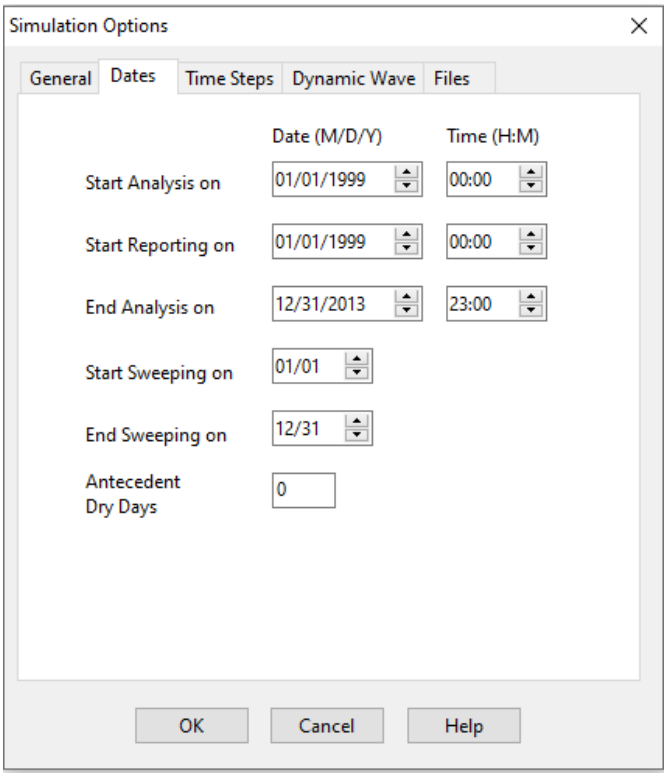

Fig. A7. SWMM model Simulation Options Dates for observed climate scenarios

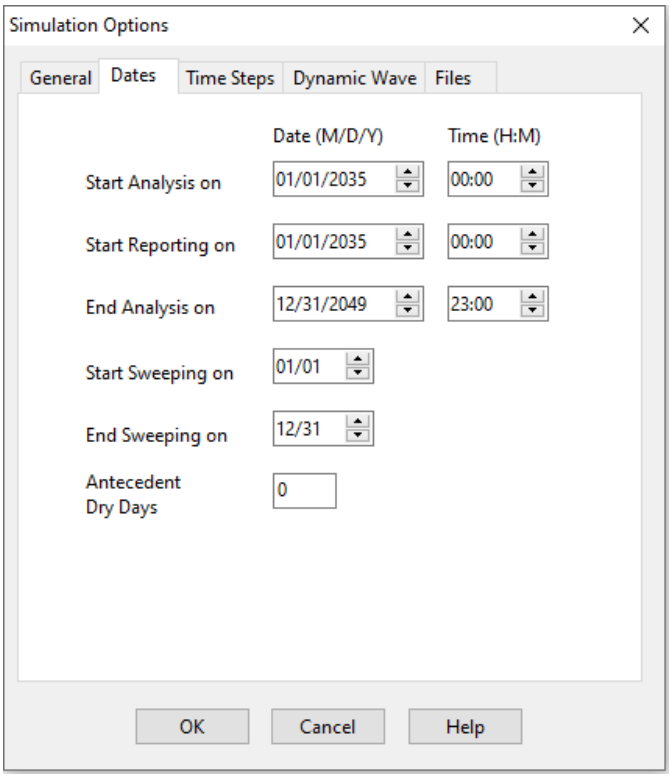

Fig. A8. SWMM model Simulation Options Dates for future climate scenarios

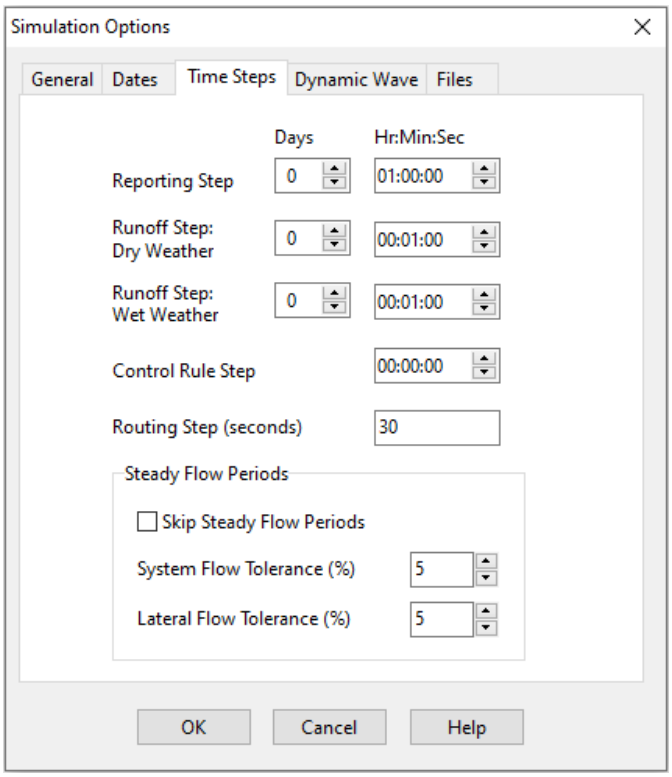

Fig. A9. SWMM model Simulation Options Time Steps tab

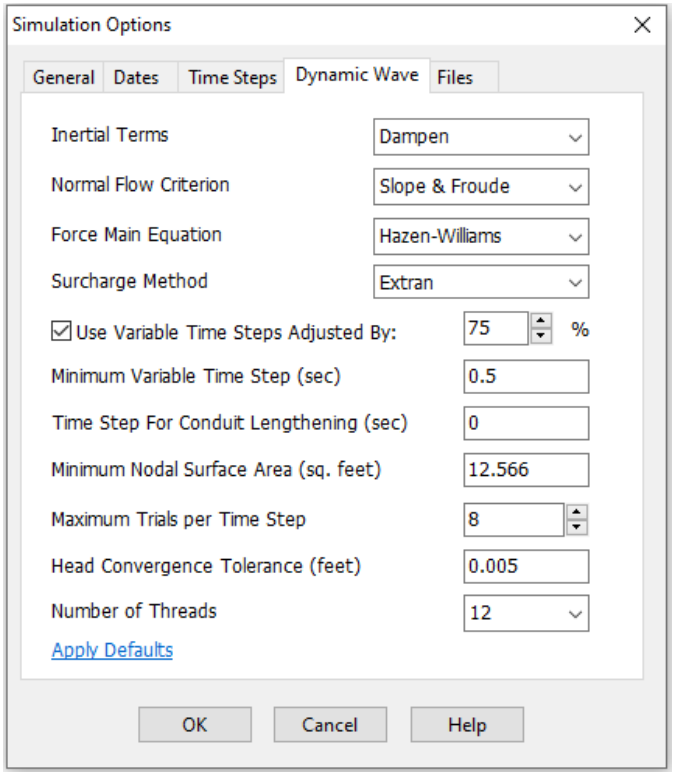

Fig. A10. SWMM model Simulation Options Dynamic Wave tab

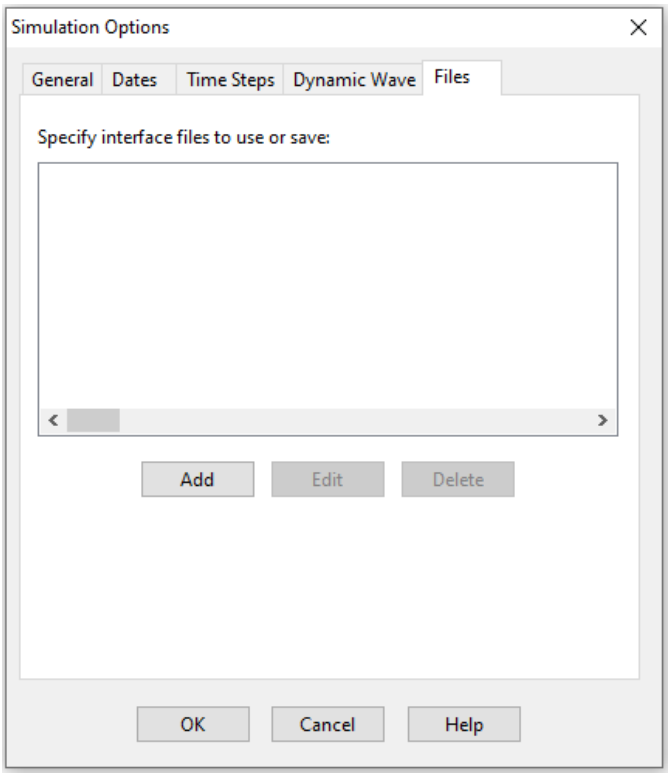

Fig. A11. SWMM model Simulation Options Files tab (none used)

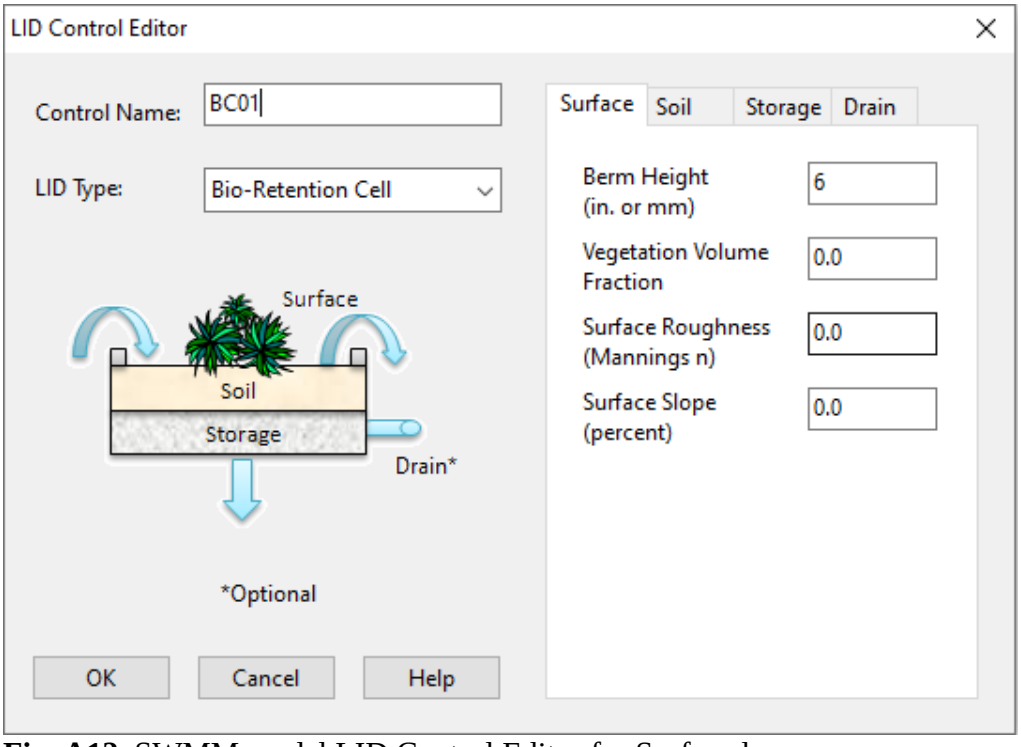

Fig. A12. SWMM model LID Control Editor for Surface layer

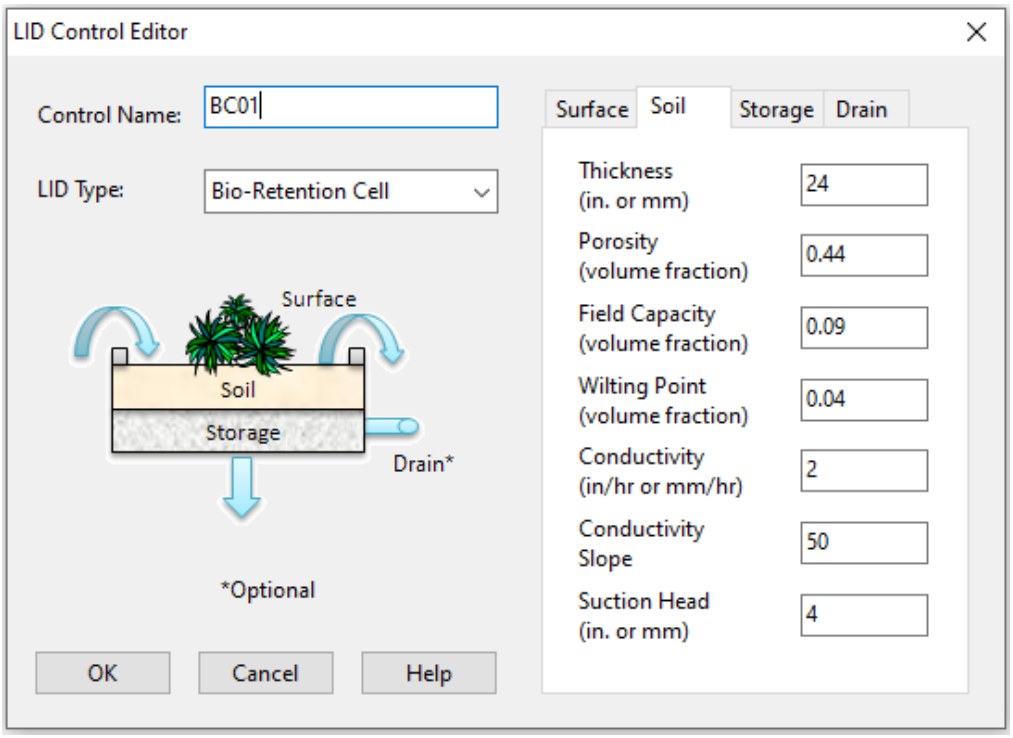

Fig. A13. SWMM model LID Control Editor for Soil layer

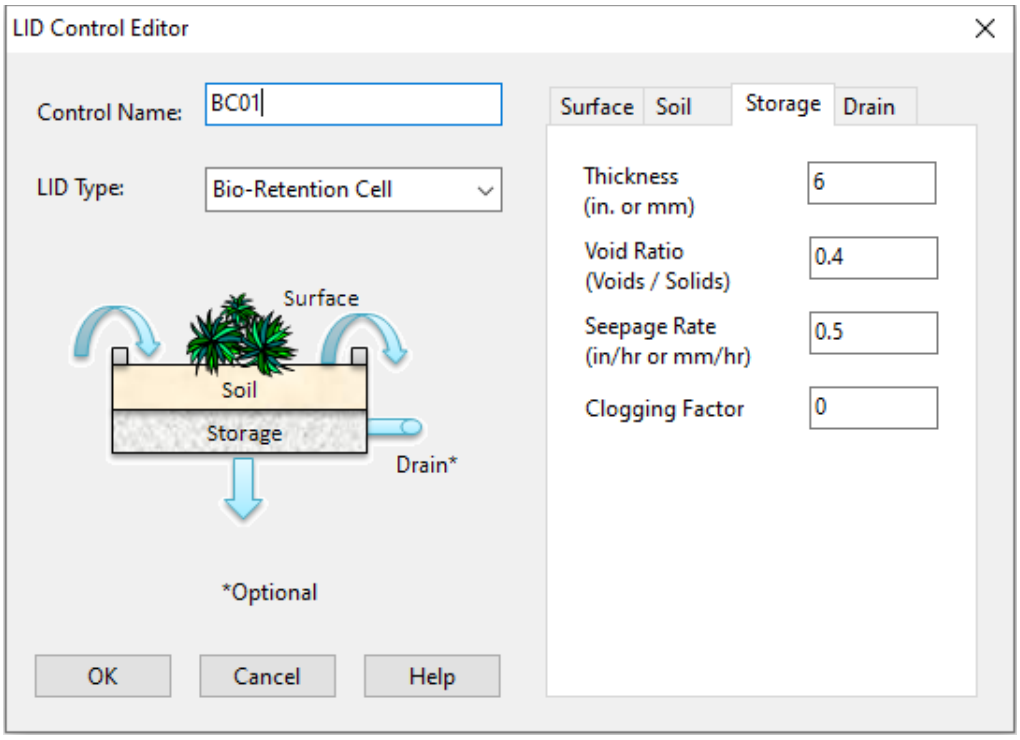

Fig. A14. SWMM model LID Control Editor for Storage layer

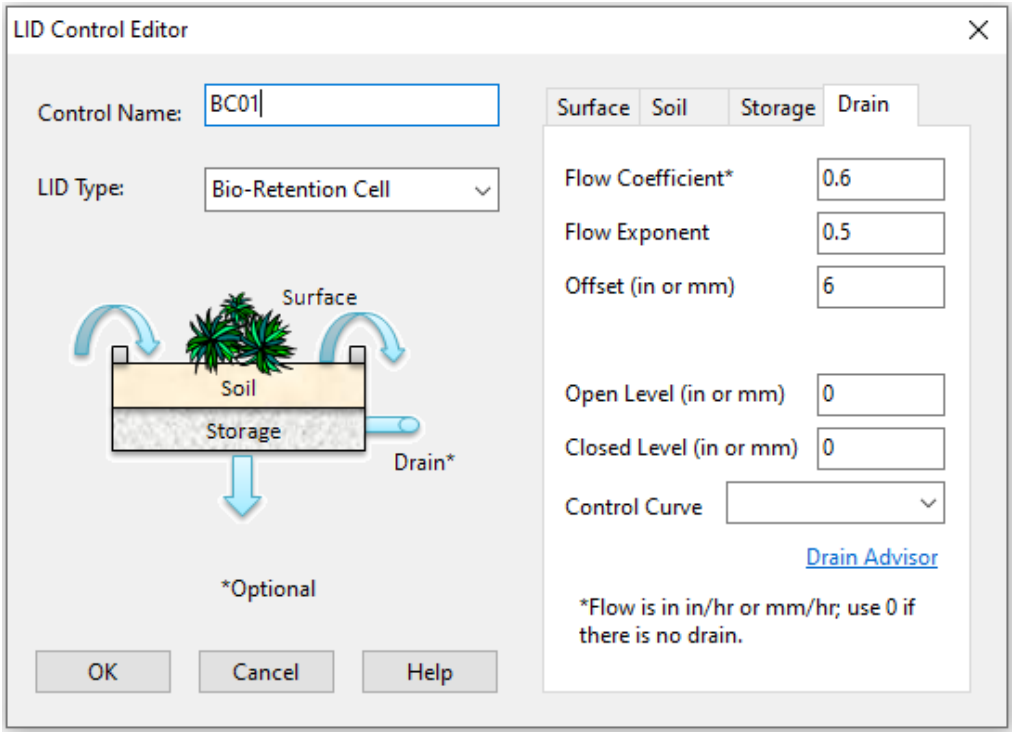

Fig. A15. SWMM model LID Control Editor for Drain layer

VITA

Originally born in Iowa, Matthew Weathers grew up in Cookeville, Tennessee. Following high school, Matthew attended the University of Tennessee, Knoxville, where he graduated magna cum laude with a Bachelor of Science in Mechanical Engineering in 2017. For the next year and a half, he performed research in the Energy-Water Resource Systems group at Oak Ridge National Laboratory in Oak Ridge, Tennessee. He then returned to the University of Tennessee, Knoxville, to pursue his Master of Science degree in Environmental Engineering with a concentration in Water Resources Engineering in 2019.